

1-1-1995

Design and implementation of an automation scheme for an eddy current scanning system

Chetan Narasimha Hebbalae
Iowa State University

Follow this and additional works at: <https://lib.dr.iastate.edu/rtd>

Recommended Citation

Hebbalae, Chetan Narasimha, "Design and implementation of an automation scheme for an eddy current scanning system" (1995). *Retrospective Theses and Dissertations*. 18280.
<https://lib.dr.iastate.edu/rtd/18280>

This Thesis is brought to you for free and open access by the Iowa State University Capstones, Theses and Dissertations at Iowa State University Digital Repository. It has been accepted for inclusion in Retrospective Theses and Dissertations by an authorized administrator of Iowa State University Digital Repository. For more information, please contact digirep@iastate.edu.

**Design and implementation of an automation scheme for an eddy current
scanning system**

by

Chetan Narasimha Hebbalae

**A Thesis Submitted to the
Graduate Faculty in Partial Fulfillment of the
Requirements for the Degree of
MASTER OF SCIENCE**

**Department: Electrical Engineering and Computer Engineering
Major: Computer Engineering**

Signatures have been redacted for privacy

**Iowa State University
Ames, Iowa**

1995

TABLE OF CONTENTS

ACKNOWLEDGMENTS.....	iv
1. INTRODUCTION.....	1
1.1 Automation.....	1
1.2 Nondestructive Evaluation and Automation.....	3
2. EDDY CURRENT BASED NDE.....	7
2.1 Eddy Currents - Basic Principle.....	7
2.2 Measurements.....	8
3. THE TESTBED SCANNING SYSTEM	12
3.1 The Scanning Process.....	12
3.2 The Scanning Hardware	15
3.3 Need for Automation.....	22
4. AUTOMATION OF THE TESTBED SCANNING SYSTEM.....	24
4.1 Inspection Process - System Components.....	24
4.2 Scan Automation Components	28
5. DEVELOPMENT OF THE TESTBED POST-PROCESSOR.....	33
5.1 Kinematics - Basic Theory.....	33
5.2 Symbols and Notation	41
5.3 Design of the Motion Automation Algorithm.....	42
6. ALGORITHM TESTING AND SCAN RESULTS.....	57
6.1 Experimental Evaluation of the Motion Algorithm.....	57

6.2 Scan Results and Evaluation.....	60
7. SUMMARY AND CONCLUSIONS	65
7.1 Suggestions for Future Work.....	66
BIBLIOGRAPHY	68

ACKNOWLEDGMENTS

This work is part of a larger team project and I would like to express my sincere gratitude for the help and cooperation I received from all the concerned members during the course of this work.

My sincere thanks to Mr. John Moulder, Dr. Norio Nakagawa, Dr. Doug Jacobson, Dr. Prasant Mohapatra and Dr. Elgin Johnston for their guidance, support, participation on my graduate committee and for their helpful comments.

I would also like to acknowledge the cooperation and support provided by my fellow team members in this project. Special thanks are due to Radhir Atthivarapu, Daksh Lehter, Aaron Turnbull, Scott Bilas and Vivek Gadiyar who all worked with me on this project.

This work was sponsored by NIST under cooperative agreement #70NANB9H0916 and was performed at the center for NDE, Iowa State University.

1. INTRODUCTION

1.1 Automation

Automation is a vast multi-disciplinary field where the advances and progress in the technology of one branch of knowledge is brought to bear on another field, creating advances and enhancements in the latter field. It is a branch of engineering that seeks to improve task efficiency by utilizing machines programmed to perform tasks that either cannot be performed (efficiently or otherwise) by humans. More generally, automation is often identified with the “computerization” of repetitive, time consuming or calculation intensive tasks that if not automated result in loss of accuracy, increasing time overheads and overall decrease in operational efficiency¹. Thus, the overall philosophy remains the utilization of machines to perform a given task so that the objective of “better efficiency” may be obtained.

Early automated systems were essentially mechanical devices. These systems were often not flexible and were designed to perform only a certain set of well-defined tasks. The main components of such systems usually included hydraulic devices, cams and levers. They could not be reconfigured or modified beyond some minor changes to enable them to perform distinctly different tasks. With the introduction of relays and motors, the performance of these systems with regard to operational time decreased. However, the latter components still did not provide the ability to program the machine or system to perform distinct tasks. The

¹ The definition of efficiency is subjective to the particular field and area of work. It is used here in a general sense.

current phase in automation is often traced to the introduction of electronic components into systems that were formerly mechanical. Vacuum tubes, formed a part of the first “electronic control systems” and provided a degree of programmability and superior performance while occupying less space and consuming less power than the earlier mechanically automated systems. The early application of computers to automation was the class of analog computers. They were often employed off-line to study and process raw data (especially in scientific institutions) and in performance simulation. The high cost and the large size of such systems, precluded their use as an embedded controller in a vast majority of scientific and industrial instruments and machines. However, in the last two decades, the single most important factor that has brought ease of use, greater control power has been the rapid evolution in the field of microprocessors. Operating on digital logic, the microprocessor has brought “intelligence” to machines.

Microprocessors and associated systems, make possible the acquisition, storage and treatment of a large quantity of information in a short time period. The superior speed of these logic devices make them an especially sought after commodity in the automation field to implement system automation schemes. Microprocessor based systems, because of their generic architecture and computing power are widely used in many of today’s instruments. The incorporation of such devices on instruments allows one to program the instruments and thus increase the capabilities of the instrument. Further, the rapid advances in software have also contributed to making microprocessor based systems more generic, flexible and powerful.

Usually, instead of building automatic systems with raw microprocessors from the bottom a microprocessor-based system, such as a computer, may be used. With computers

becoming more powerful and compact, automation has come to rely more on the power of software than ever before. The latter allows more flexibility and ease of use in building and maintaining an automated system.

With the development of “virtual instrumentation” (in the late 1980s) the flexibility and power of disparate instruments can be homogeneously used to achieve a task objective. Virtual instruments allow one to build a complete instrument implemented in software while using relatively simple and cheaper devices to do the actual data acquisition. It also allows the seamless integration of different devices so that the integrated device combines the features of all these instruments and presents a uniform interface to the user. Also, the rapid advances in computer to computer communication systems have led to networked systems spread across the geographically separated sites. Networked instruments allow efficient communication and retrieval of information. Thus, the available resources are utilized efficiently to serve a given objective (for example, Supercomputers are often utilized for information processing while the instrument that collects the information itself is a geographically separated, distinct entity).

1.2 Nondestructive Evaluation And Automation

Materials and manufactured products are often tested prior to delivery to the user to ensure that they will meet expectations and remain reliable during a specified period of service. A testing of the product that in no way impairs or changes the properties of the product is called nondestructive testing (NDT). Very often such testing is crucial at the manufacturing stage and/or during product service, especially if the product failure leads to

possible loss of human life, damage to the environment, etc. Structures and components used in aircrafts, nuclear installations, etc. are often subjected to heavy stress, fatigue and corrosion. As a result, defects such as such cracks are likely to form and grow. NDT techniques are often employed in studying such structural changes, defect initiation and growth. Such study utilizing NDT, is often referred to as nondestructive evaluation (NDE) [Blitz].

Manual operation of NDT methods has the advantage that the operator is in a position to make immediate decisions when proceeding from one stage of testing to another. This determination by the operator requires skill and technical knowledge that is acquired by formal training and experience. Often however, the inclusion of the human element results in such advantage being gained at the cost of time and risk of human error. If multiple channels of information are present, then such analysis in optimum time frames becomes extremely complex and inefficient for the human operator to perform. A well-defined automation scheme helps in efficient information collection, processing and output. In addition, it very often helps improve experiment repeatability and stricter experiment parameter control while not sacrificing accuracy. With advances in neural networks and AI it is also often possible for the system to “learn” from the human operator and perform the same task. Further, with the presence of embedded computers and dedicated control it is possible to incorporate some form of fault tolerance and recovery. Such features are driving automation systems towards a more “smart” future.

1.3 Aim and Scope of this Work

Eddy current scanning is highly sensitive to the relative position of the probe to the component under scan. Ensuring that the probe maintains a constant lift-off and is perpendicular to the surface being scanned is of great importance to the scanning process, as the signal strength is best under the above constraints. Earlier work on scan automation attempted to use the probe signal to control the lift-off variations (which are an important source of noise) so that a constant lift-off could be maintained over a non-planar complex surface[Bugar].

This work focuses on developing a systematic method to,

- achieve probe perpendicularity and constant lift-off all through a given scan, in order to obtain accurate and repeatable eddy current measurements.
- eliminate the time overhead present in developing motion control software that is specific to a given geometry, so that we have one generic method or algorithm to scan objects having any given geometry.

To attain these objectives an automated scanning system was developed that would integrate the scanning process from scan conception to scan realization. A key component of this automated scanning process (and the main focus of this work) is the development of a postprocessor algorithm to realize in practice, the scans generated (at the conception stage) in software. This work is organized in the following manner.

Chapters 2 through 4 provide the introductory and background material. Chapter 2 describes the basic concepts of eddy current theory and its utilization in nondestructive

evaluation of metals. Chapter 3 describes the existing scanning (or inspection) hardware (called the Eddy Current Testbed) upon which the new automated system was developed and describes the issues involved in automating the scanning process. Chapter 4 describes the overall eddy current inspection process and the experimental module of this inspection process (whose automation is the focus of this work).

Chapters 5 and 6 address the specifics of this work. Chapter 5 provides a brief theory of kinematics and then proceeds to describe the postprocessor algorithm that allows the existing hardware to conduct the complex scans generated first in software. Chapter 7 presents a summary of the work, the conclusions arrived at and suggests possible enhancements and/or modifications for future work.

2. EDDY CURRENT BASED NDE

The eddy current method of nondestructive testing, as currently practiced, was pioneered by Fredrich Forster in the 1940s and there has seen rapid progress in its development. Eddy current tests can be made on all materials that are electrically conducting. They include the sizing of surface and subsurface cracks, measurements of the thickness metallic plates and of non-metallic coatings on metal substrates, assessment of corrosion and measurements of electrical conductivities and magnetic permeabilities. An important advantage of eddy current testing, is that there is no need for physical contact with the surface of the objects being scanned. Thus, careful preparation (other than the removal of mechanical adherents) is unnecessary.

2.1 Eddy Currents - Basic Principle

The practice of eddy current testing, consists of exciting an alternating current at given frequency through a coil, often called a probe-coil or simply a probe, located as near as possible to the electrically conducting object being tested, and thus induces eddy currents in the latter. As a result, changes take place in the components of the impedance of the coil which can be related to the design of the coil, the size, shape and position of the test object and the values of its magnetic permeability (μ) and conductivity (σ). The impedance of the coil is also affected by the localized variations in μ , σ and the geometry of the object under test as a result of the presence of the defect.

With the eddy current method, the current passing through the coil generates electromagnetic waves through an electrical conductor in its vicinity. The associated magnetic field H induces the flow of electric currents, i.e. eddy currents, which follow circular paths in planes perpendicular to the direction of H , in accordance with the below equation

$$\text{curl } H = J \quad (2.1)$$

where J is the current density. The coil and the metal sample form respectively the primary and the secondary components of a transformer, and the impedance of the coil is consequently affected by the behavior of the eddy currents. Neglecting the ohmic resistance of the coil, this impedance at a frequency $\omega/2\pi$, is purely inductive and has a value $Z_0 = j\omega L_0$, when completely removed from the test object and any other electrical conducting and ferromagnetic materials. When the coil is located in the testing position, the value of the impedance changes from L_0 to L and a resistive component R is introduced. The changes in the impedance components are determined by the speed and the attenuation coefficient of electromagnetic waves in the test sample and the corresponding phase changes in the relevant electrical and magnetic vectors, i.e. B , H and J are responsible for introducing the component R of the impedance.

2.2 Measurements

The probe coil arrangement has a distinct effect on eddy current measurement. In general there are three possible coil arrangements namely encircling for tubes and rods, internal axial for tubes and surface scanning. The latter are used for testing surfaces which are

either plane or have very small curvature within the region directly below the cross section of the coil. For enhanced sensitivity, transformer probes, which have separate transmitting and receiving coil windings may be used if, deep penetration of eddy currents is required in the material under test. Prior to any eddy current testing , a calibration should be made with a standard sample. If it is free from defects, the relationships between the impedance of the components of the coil, the frequency and the electrical and magnetic properties of the material can often be obtained theoretically.

The essential parts of eddy current equipment are the exciting oscillator, the measuring circuit, usually an AC inductance bridge, and the detecting coil (or coils). The object is scanned either manually or with the aid of a mechanical device. Eddy Current testing determines the components of either the impedance of the detecting coil or the potential difference across it. Most applications require determinations of only changes of impedance, which can be measured with a high degree of sensitivity with an AC bridge (Fig. 2-1). The principle of operation of most commonly used eddy current instruments is based on Maxwell's inductance bridge. In the bridge circuit, the impedance components ωL_3 and R_3 are compared with the known variable impedances, R_4 and ωL_4 connected in series and forming the balancing arm of the bridge. If R_1 and R_2 are the ratio arms, the balancing condition is given by ,

$$R_1/R_2 = R_3/R_4 = L_3/L_4 \quad (2.2)$$

where, R_1 and R_2 are fixed resistors and equal to one another while inductance L_4 and impedance R_4 are variable.

It must be noted that test circuits vary greatly depending upon applications. Some instruments also incorporate lift-off compensation, which essentially reduces the sensitivity of the signals to lift-off variations. This reduction in sensitivity is achieved locating the frequency at which the sensitivity to lift-off is a minimum. The input EMF to the bridge circuit is an AC oscillator, often variable in both frequency and amplitude. The highest sensitivity of detection is achieved by properly matching the impedance of the probe to that of the measuring instrument. Thus, with a bridge circuit which is initially balanced, a small variation of the probe's impedance upsets the balance and a potential difference appears across the detector arm of the bridge. The detector arm of the bridge circuit takes the form of either a meter or a

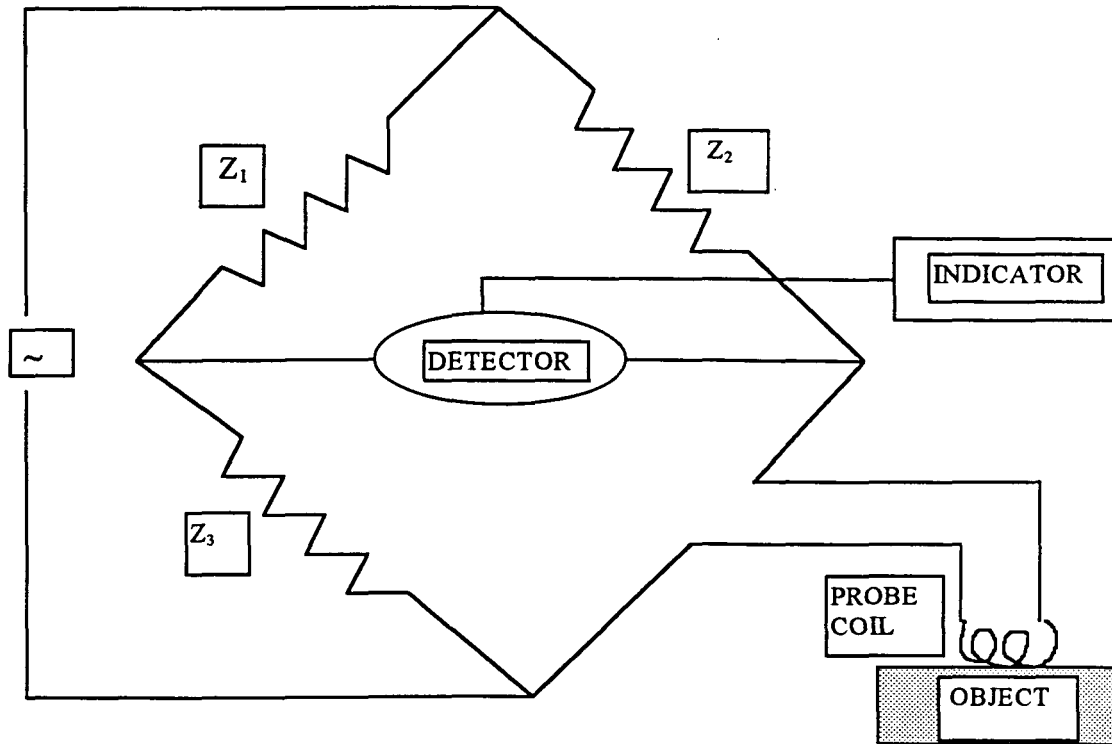


Fig. 2-1: A typical bridge circuit

storage cathode-ray oscilloscope, a phase-sensitive detector, a rectifier to provide a steady indication and, usually, an attenuator to confine the output indication within a convenient range. Many detectors also incorporate storage facilities. Instruments like the HP4194A Impedance/Gain Phase Analyzer also incorporate communication features that allow the instrument to communicate with other instruments using the HP-IB protocol (IEEE 488.2 standard), in addition to a multiple feature detector arm that allows the data to be viewed in more than one form..

3. THE TESTBED SCANNING SYSTEM

3.1 The Scanning Process

Eddy Current scanning is highly sensitive to the relative position of the probe to the component (or the object²) under scan. The signal strength is dependent on the relative tilt of the probe to the object's surface being scanned. The signal is best when the probe is oriented perpendicular to the surface being scanned. The signal is also dependent on the lift-off of the probe from the surface. To scan a surface the probe is held at a given point on the surface and measurements taken. The measurement (usually an impedance value) is very sensitive to the orientation of the surface w.r.t the probe tip; For the best possible detection of flaws the probe should be preferably, perpendicular to the surface at the scan point. Maintaining the orientation and the liftoff at all the scan points (when a subset of the object's surface is scanned) is crucial if one seeks to detect small flaws (say, of the order of 10 ~ 30mils). If the probe orientation and lift-off vary as the scan proceeds over the surface then it becomes difficult to separate the changes in impedance that occur as a function of liftoff from the changes in impedance due to the presence of the flaw. Thus, the flaw is effectively hidden in the data and it is a complicated task to extract the flaw signal from the scan data in such cases where the lift-off and orientation parameters are not maintained at a constant value. The task

² Component, object or sample all refer to the object being scanned by the probe and are used interchangeably.

of maintaining a constant lift-off and a constant orientation of the probe, is a relatively easy in the case of scans over flat plates, but becomes a non-trivial problem if the scanned surface has a geometry that incorporates second order or higher curves. As is evident positioning of the probe while maintaining a strict control over the above two parameters is not an easy task in such cases and calls for a good positioning apparatus. Precise control of the probe in such cases, in a laboratory environment is achieved by using motors (usually micro-stepped steppers) to achieve fine scan resolution.

Some common scans that are performed include, a “raster scan” where the probe motion is similar to the electron scans on the television. This is also similar to the one-way cut executed on milling machines. Here, the probe traverses the surface, collecting data, in a constant direction. Once a line of scan is complete the probe moves back to the start point of the current line and then steps to the next line.(in the perpendicular direction). Thus, the data collected can be considered conceptually, to be a two dimensional matrix of $m \times n$ points with say, m lines and n points in each line (Fig. 3-1).

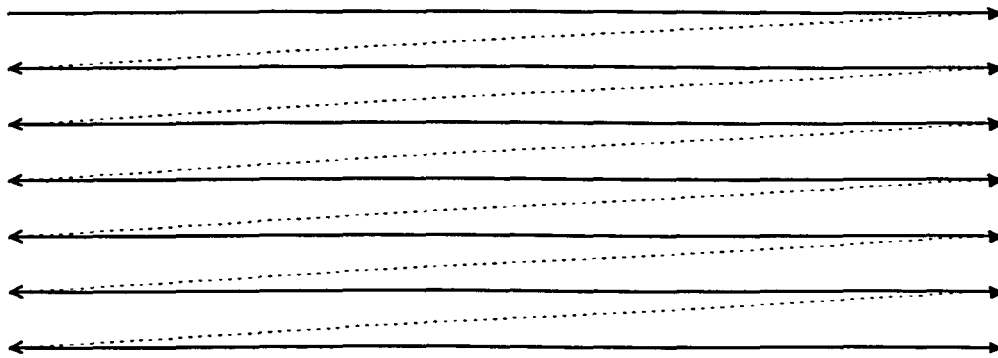


Fig. 3-1: A raster scan ($m = 7$ and n points per line)

Thus a “surface of points” is obtained and corresponds to the surface scanned. Depending on the special nature of the geometry the scan may be circular etc. In each case the parameters that affect probe impedance are to be controlled and maintained at a known value, so that the data is principally affected by the flaw alone.

In the laboratory environment, the probe’s positioning can be effected by motors whose motion is controlled from a programmable device (most stepper motors come with a manufacturer provided controller and a Motor driver). In many cases the place of the programmable device is taken by a dedicated computer running a custom developed scanning software that positions the probe or moves the probe while collecting the data. The sequence of Motor motion etc. is all determined by the software (program) written to scan the specific object’s surface as desired by the experimenter. In the case of say, a raster scan over a flat plate, the program (or programmer) specifies the Motor to move so that the probe travels along a straight line. The program specifies the step size, the place to stop and make a measurement etc. and the point at which to step on to the next parallel line (The initial lift-off and orientation once set are not affected appreciably in this scan as the motion is only in a flat plane).

As is evident the scanning process tends to increase in complication as the surface to be scanned becomes more complicated in its geometry. It is precisely this problem that is sought to be addressed in this work. The following chapter gives a description of the hardware components that work in tandem to execute a scan (“scan realization”). The next chapter describes the problem hinted at briefly at the beginning of this paragraph.

3.2 The Scanning Hardware

This chapter describes the hardware arrangement that aids in the actual execution of the scan. The Eddy Current (EC) Test Bed Station (called ECTB) serves as the hardware platform for the scan execution. It is built around a computer controlled measurement workstation and is designed to achieve precise, repeatable EC measurements on parts with even 3D geometry. The three main components of the scanning hardware comprising the ECTB are,

- A positioning system that actually positions the probe over the surface of the object being scanned.
- A data acquisition unit that performs the functions of exciting the probe coil and collecting the impedance value at that point.
- A dedicated computer functioning as a controller. The computer is an in loop computer that commands the actual task sequence, collects the data and helps in data processing(in an off-line mode).

Fig. 3-2 provides a schematic of how the data are linked together.

The following sub-sections describe each of the above scanning hardware components in greater detail.

3.2.1 The Positioning Hardware

The positioning hardware consists of two sets of four axis machines, each having its own Motor controller. The Motor controllers can function either in a stand alone mode or in a remote mode. Each of the Motor controllers can control upto four stepper motors. Each of

the axis is controlled by a stepper Motor The stepper motors have a position feedback mechanism (an encoder³) that allows the corresponding controller to function in a closed loop mode. Thus, each command (command steps) is checked against the steps moved by the Motor and the controller corrects any error. Section 3.2.1.1 provides more detail.

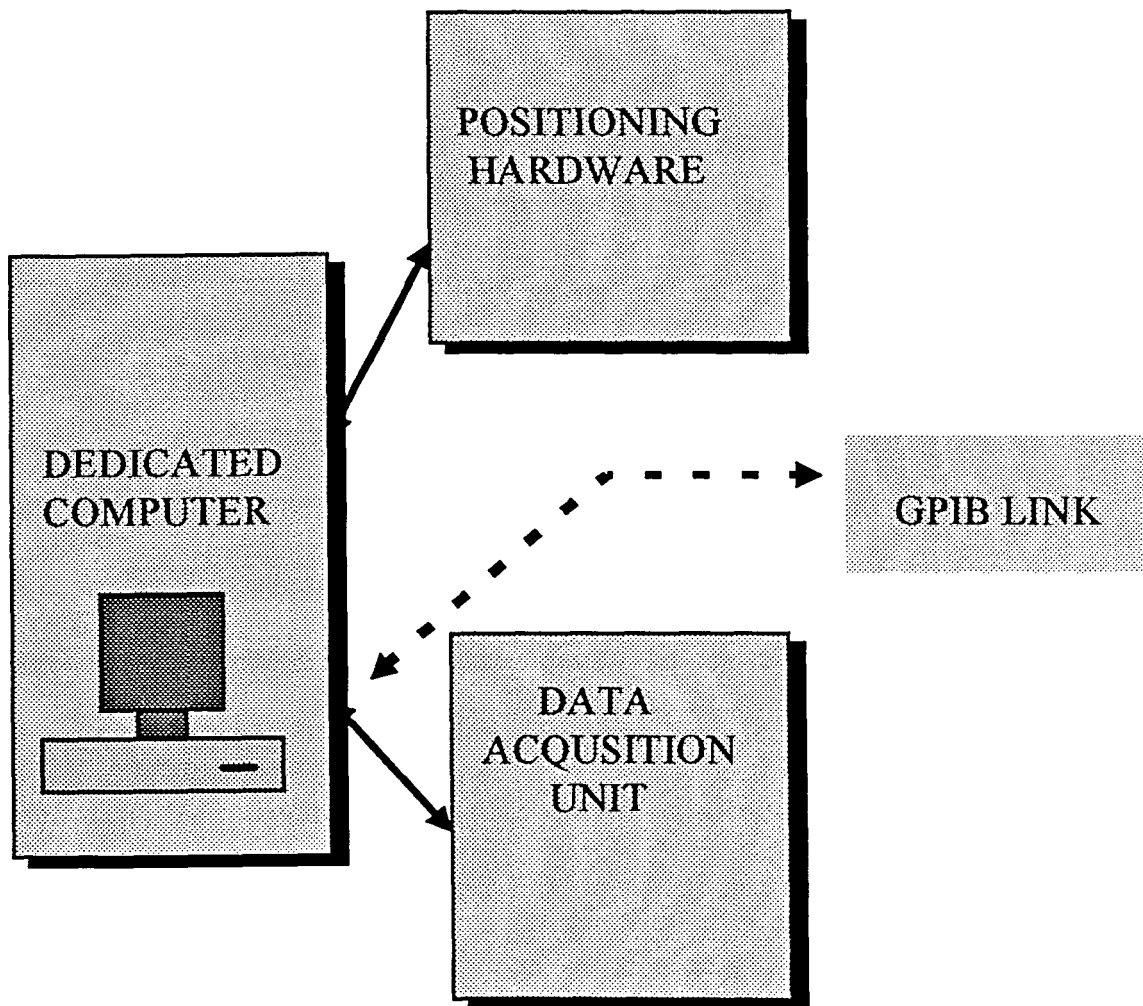


Fig. 3-2: scanning Hardware - components

³ Optical encoders.

3.2.1.1 The Motor Controller

The controllers are Compumotor's, 'Model 4000 Motion Controllers controllersTM'. Each controller can function in an off-line stand alone mode where it executes a program previously downloaded to it by a serial or a parallel link (RS 232-C or GPIB) (Fig. 3.3). The Motor controller has the following features:

- Menu-driven operation.
- A BASIC like motion control programming language that works from the controller and another command driven language that is used to control the controller from a remote site.
- A teach mode using analog joy-sticks or operator panel jog sticks.
- A non volatile battery backed RAM (16K ~ 64K)
- Optional contouring and IEEE -488 standard features.

The controller is a microprocessor based controller running a M68000-12Mhz processor. The controller has separate drive and encoder ports. The controller, as described above, allows command execution in a downloaded mode or in an immediate execution mode. In the downloaded mode the program commands are entered on a computer (a remote unit) and then down loaded to the controller via an RS-232C or a GPIB link. These commands are defined in the manufacturer provided custom programming language, called the MC4000 Command language. Commands may also be sent one at time The latter feature has the advantage of allowing the computer to track the motion etc. but suffers from the disadvantage of tying up the computer (This can be overcome if the operating system allows process multi- threading,

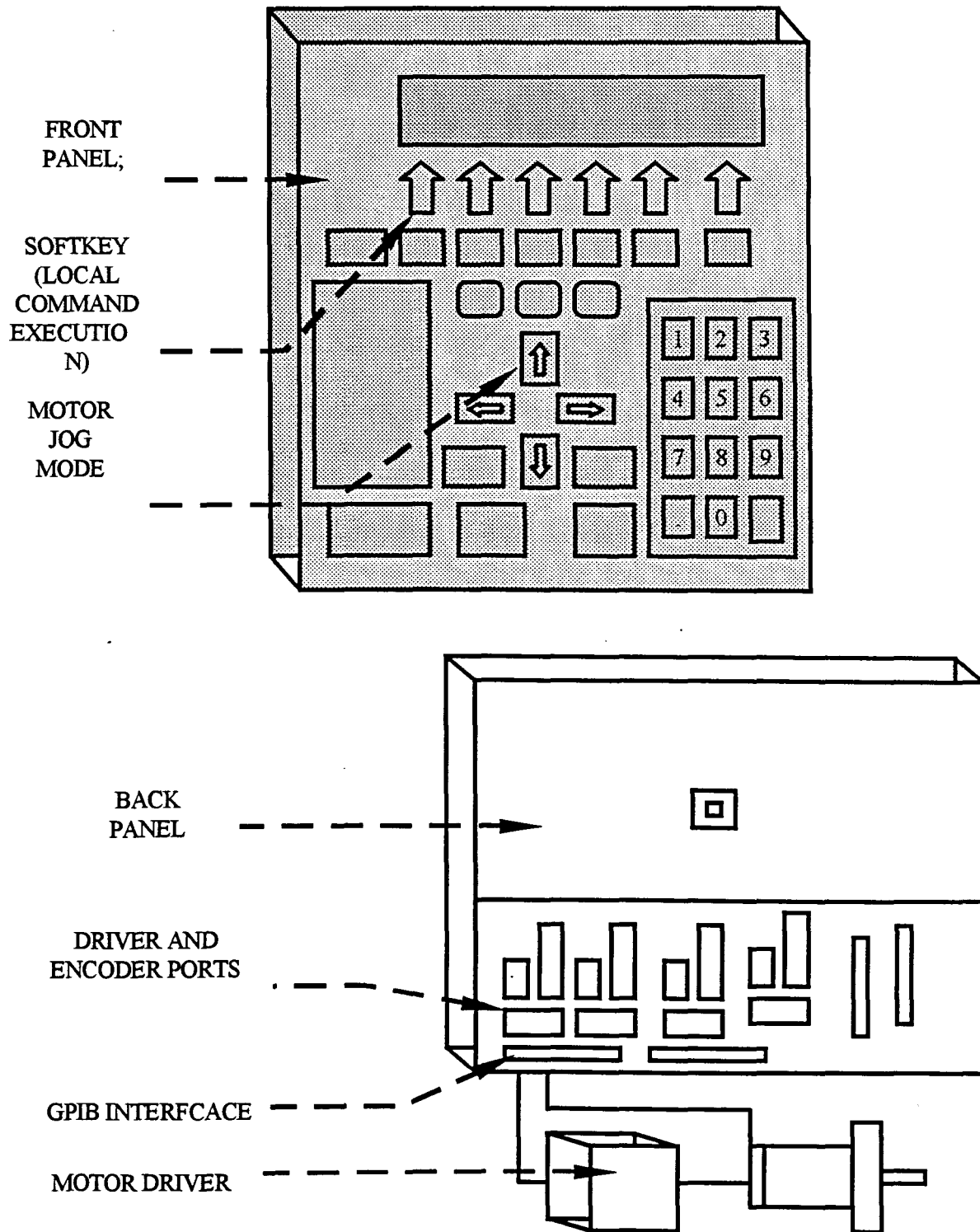


Fig. 3-3: The MC4000 Controller

as in UNIX/WIN, NT, so that one process does not tie up the computers resources - as in DOS and WIN 3.1). The remote command language provided is the X command language. The X command language allows interactive operation of the individual axis in an independent manner, as though the four axis were controlled by four individual controllers, tied through a daisy chained serial link. There are no global commands.

3.2.2 The Hardware Arrangement

The probe is mounted on one of the machines and the object is either mounted on the other (if physical considerations permit such a mounting) or is placed on the underlying table surface. The probe and object arrangement is as shown in Fig. 3.4. This arrangement lends each of the entities (probe and the object) the maximum possible degree of freedom of motion. The probe and object machines are controlled by their individual controllers, that are in turn controlled remotely by a dedicated computer that acts as the GPIB controller for the whole system. The computer also controls the data acquisition instrument (The HP4194A). All the instruments run the GPIB protocol providing a standard communications interface.

3.2.3 The Data Acquisition System

The data acquisition system show in Fig. 3.2 is an HP4194ATM Gain/phase Impedance Analyzer. It is a sophisticated instrument with the ability to acquire, display and analyze the data, being controlled from the control panel or from a remote instrument. It runs the HP-IB communication protocol which agrees in standard to the IEEE 488.2 instrument protocol. The Impedance analyzer acquires the data in an analog form and internally process the data and

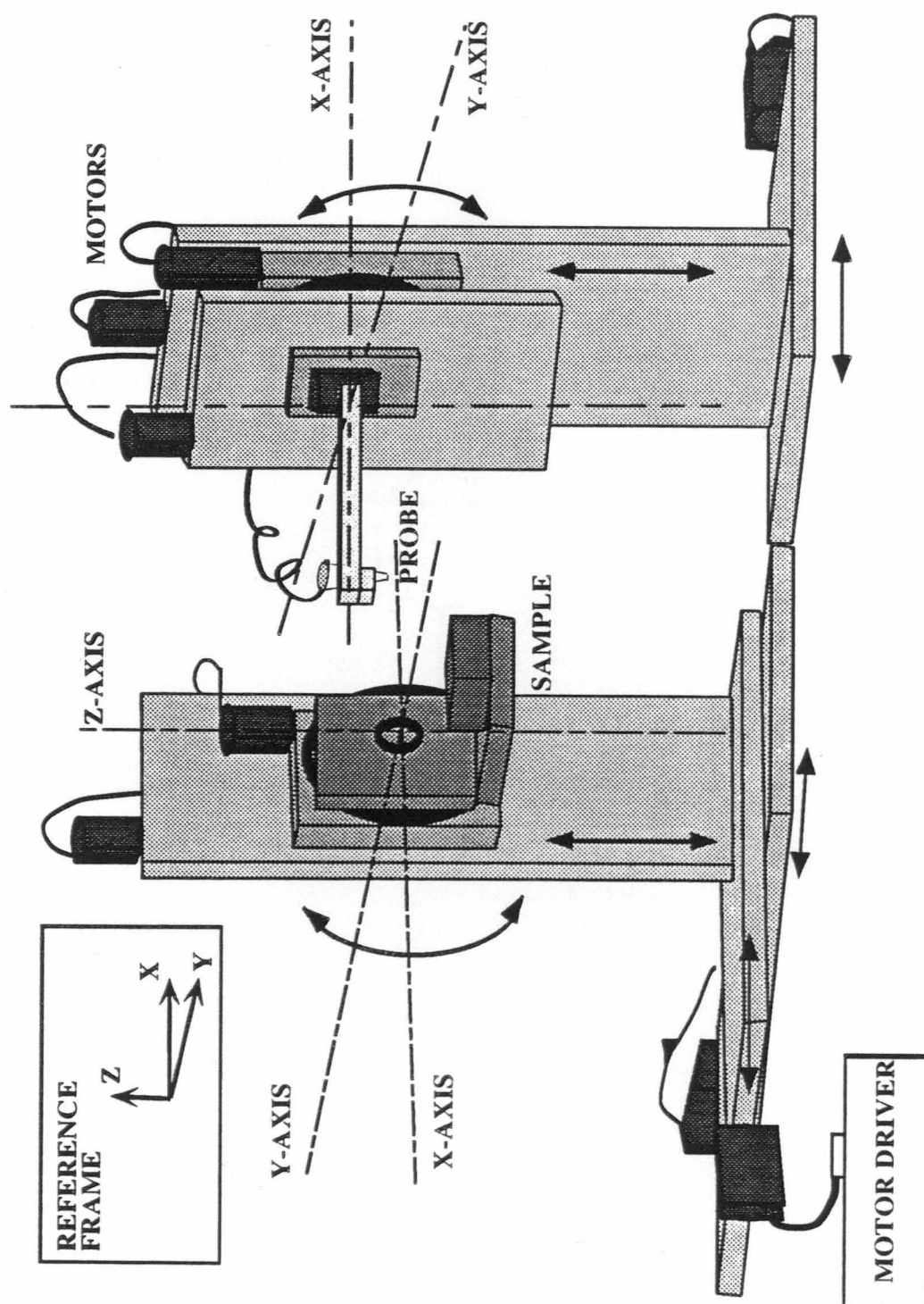


fig. 3-4 : Schematic of the positioning hardware

stores it its internal registers in a digital format. The data is available on demand to remote instruments, controllers etc. It has features for multi-frequency scans and facilities to control the averaging and integration times for each scan data that is obtained; There are 3 integration times (Small, Medium and Long) and the number of averages can range from 2^1 to 2^{256} .

The HP4194ATM feature eleven Impedance and four Gain-Phase measurement functions and covers a frequency range of 100 to 40MHz for Impedance, and from 10Hz to 100MHz for gain-Phase. The output level, with an adjustable dc bias level of $\pm 40V$, ranges from 10mV to 1Vrms for Impedance and from -65dBm to +15dBm for Gain-Phase. The basic accuracy is 0.17% of impedance and 0.1dB/0.5° for Gain-Phase.

The 4194A's menu-driven software uses eight softkeys located next to the menu are of the CRT (Cathode Ray Tube). This allows, the instrument to be programmed from the front panel. Measurements inside the 4194A is stored as complex data. Using this storage technique and the math processing capabilities of the 4194A, several display formats may be derived from the same trace data and changes in scale may be made without repeating the measurement.

3.2.4 The Instrumentation System Controller

The Controller is a dedicated IBM PC compatible computer controlling the positioning and data acquisition systems. The controller functions in-loop, essentially in a feedback mode and verifies each scan state for its validity. The instrument interface used is the National Instrument's NI-488.2TM GPIB interface.

Thus far, the controller utilized the MS-DOSTM and the WIN. 3.11TM operating systems. Since these operating systems are not multi-tasking systems, the computing resource is essentially tied up while the system is in operation (scanning and collecting data). Further, these operating systems also do not provide good process security and hence have a tendency to crash the controller in case the individual software malfunctions. In order to overcome these limitations, the controller software is being ported over to the new 32 bits WINDOWS NTTM platform, which provides multi-threading and better process security. It is better suited to handle distributed client-server computing, towards which the automation system could move. Further, it provides upward compatibility to software developed under WIN 3.11 and MS-DOS, thus easing the transition to a more powerful system

3.3 Need for Automation

The above chapters provided a background to the main focus of this work. As was seen, the Eddy Current scanning process is very sensitive to variations in its lift-off and the signal can also vary depending on the orientation of the probe to the object surface. The probe signals are at their best when the probe is perpendicular to the object. If this is not the case, the probe signals will vary depending on the orientation of the probe to the surface. Thus, a strong background component is introduced into the overall signal data. This background inclusion makes the immediate detection of flaw signals a more complicated task. Hence the experimenter must take care that the positioning system attempts to place the probe in a position as perpendicular to the object as is possible. In cases, where the object scanned is a

flat plate or a cylinder etc. programming the probe motion is a relatively simple task. Here, the programmer (or the experimenter) is intuitively using the symmetric nature of the object geometry to determine the motions that are required to position the probe. It is immediately clear that this is a non-trivial problem in the case of an object possessing a complex curvature and that the use of intuitive ideas may not be always feasible in accurate positioning.

Developing a software that is valid only for the particular geometry at hand results in a process where each time a different object is to be scanned, a new software is developed. This results in developmental time overheads.

The above factors, thus motivate the need for more detailed information regarding the object geometry. This information can be obtained from a standard coordinate measuring machine (CMM) that scans the object surface to provide a data file containing the object geometry information. This provides a way to handle the accurate geometry information that the probe requires in order to be positioned perpendicular (or at any known orientation) to the object. It is also evident that scanning such a complicated object is more efficiently handled by a software that utilizes the coordinate information to automatically position the probe.

The above factors are essential in motivating the need for an automated scanning system, that provides a structured and standardized method of setting and executing scans. The following chapters describe the development of a system designed to achieve these objectives.

4. AUTOMATION OF THE TESTBED SCANNING SYSTEM

This chapter describes the testbed system components, first adopting a black box approach. Once the overall relationship between the individual components is established, we go into the functioning of each of the components and establish their need and their contribution in automating the scanning process. Section 4.2 provides a block diagram view of the various subcomponents that go into the eddy current scan realization process and discusses the relationship between the sub-components in the scan realization module.

4.1 Inspection Process - System Components

Figure 4.1 establishes the relationships between the various components that contribute to the Eddy Current Flaw detection and evaluation process. It must be noted that the flow of process shown, does not imply a rigid relationship, but rather serves to establish the conceptual relationship between the various components that go into the inspection process. For example subcomponents in stage VI (discussed in the next section) rely on stage II too.

- (I) The first step in the inspection process begins with the acquisition of geometry data into the computer. This data is either the result of a part designed in-house or is obtained from a part that has already been designed and manufactured. The geometry if designed is usually done with the aid of a workstation. commercial packages such as I-DEASTM, a solid modeling package, are typically used in designing and developing the part or object model. This software model is then

ported to the next stage where it is input into a Computer Aided Milling Machine Manufacturing package (CAM). Alternatively an integrated package that includes CAD (Computer aided design) and CAM can be used⁴. This has the advantage of avoiding problems associated with porting files from one computing platform to another.

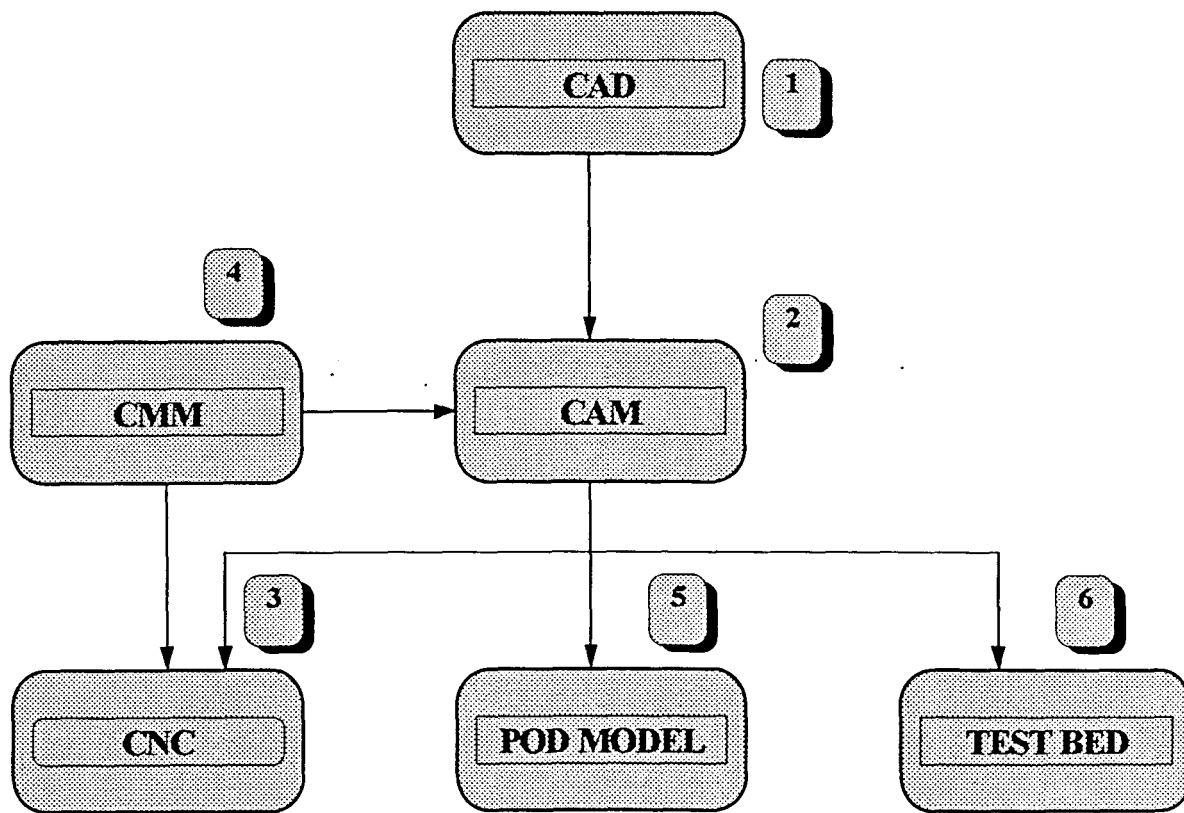


Fig. 4-1: A system layout of the eddy current inspection process

⁴ A CAD/CAM system is an integrated software tool that prepares engineering design details, finished blue prints and NC programs. The latter are used to run the CNC (Computer Numerical Control) machines that control the part manufacturing etc. They often include visualization user interface tools.

(II) This is the scan generation stage. In this stage, the component designed in stage I, is utilized in obtaining a probe path over a desired portion of the component surface. Due to the perpendicularity constraint imposed in the scanning process, the motion of the probe is not unlike the motion of a milling machine tool. It is because of this similarity that a milling machine package was chosen to aid in developing a desired probe path. The advantages of using this approach are,

- Provides visual feedback which is quick and intuitively more easier.
- Scan area selection is accurate and also easily modified if required.
- Provides the coordinate positions of the tool (also corresponds to the desired probe positions) that can be used to determine the probe motions at the scan execution stage.

(III) Once the probe motions have been generated by the CAM, it is now possible to branch into either stage III, V or VI depending on the particulars of the situation. If the component has already been manufactured and the geometry data available, then stage III and IV are essentially redundant. It is then possible to proceed directly to the scan execution stage (stage VI). Either way, a POD (Probability of Detection) Model of the flaw inspection can now be obtained after stage I and II. stages V and VI (Fig. 4-1) are essentially independent of each other. stage VI (the scan execution stage) is however dependent on stage III and IV. In stage III the part is manufactured (if not already manufactured) and then the manufactured component or object is scanned using a coordinated measuring machine (CMM-stage IV) The latter process verifies that the object has been manufactured as per

the design. A CMM verification can also be done on already-manufactured objects. This provides a valid feedback mechanism on object geometry. The next stage is the scan execution stage.

(IV) In stage VI, the scan is actually executed on the testbed. The scan execution (or the scan realization) stage utilizes the coordinates generated in stage II by the CAM. The scan execution results in data being acquired over the desired surface(selected in stage II). The scan data (obtained from the probe) is then post processed to remove noise, and any data pattern that reflects the effects of the background. There are two main components in the scan realization stage, namely,

- A post-processor stage where the coordinates of the probe motion generated in stage II, are processed so that the individual motion components (translation and rotation) of the probe (and/or the object) are determined. This determination is essential as the positioning hardware cannot execute all the possible probe motions that show on the CAM path generation. (stage II). A new set of parameters indicating the actual probe (and/or object) motions is created. This intermediate stage results in the creation of a “post processor”.
- The post processor is utilized by the machine interface software, to control the sequence of machine motions and the acquisition of scan data.

- The postprocessor is utilized by the machine interface software, to control the sequence of machine motions and the acquisition of scan data.

The following section, concentrates on stage VI (testbed) and explains the sub-components of that stage.

4.2 Scan Automation Components

There are four principal modules that are involved in the scan realization stage (stage VI). As seen in Fig. 4-2 these include,

- A scan generation module
- A testbed post processor module
- A post processor motion visualization module
- An interface software

4.2.1 The Scan Generation Module

Consider Fig. 4-2. The CAD/CAM module in Fig. 4-2 is the same module that was discussed in the preceding chapter. Given a data of the object whose surface is to be scanned by the probe, this module helps in generating a probe path over the surface to be scanned (in software). The presence of visualization tools, aid in easy selection of the probe motion and in arriving at the optimum number of scan lines etc. that are required for a good scan over the object surface. A milling machine CAM package was used and the tool positions were interpreted as the probe positions.

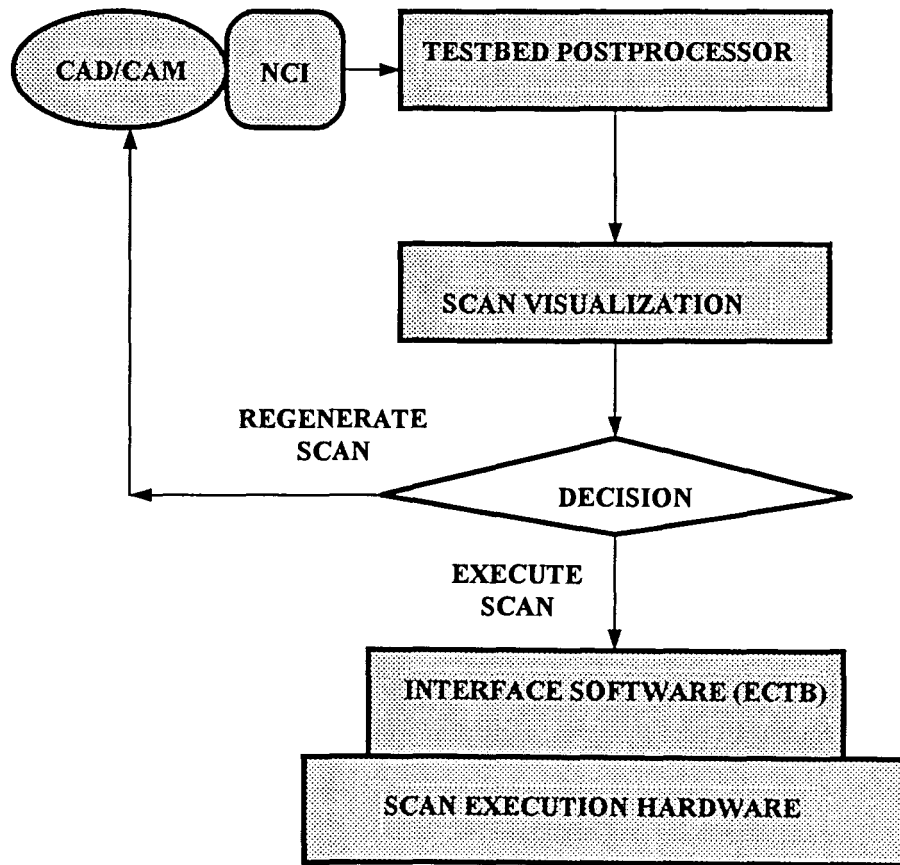


Fig. 4-2: A flow diagram of the scanning process.

Once the desired probe path is generated on the CAM station, a coordinate file called the NC intermediate (NCI) file is generated. This file describes the coordinates occupied by the probe's tip and center in 3D space at each of the scan points. A typical NCI file is shown in Fig. 4-3. The headers of the NCI file are shown bold. The parameters corresponding to the headers follow in a line directly below (Please see Fig. 4-3 which shows a representation of the NCI file). The headers represented by the numbers "11" are the scan points. The eight parameters that follow below the header represent the six coordinate positions, and a velocity and scan point status indicator (shown double underlined). The numbers are standard and pre-

double underlined). The numbers are standard and pre-defined by the manufacturer. For e.g., 12 represents the *Start of scan* , 22 the *Middle of scan* and 32 the *End of scan*. Thus the NCI file provides the raw data that describes the motion of the probe over the object's surface in 3D space.

1001		<Header - Start of File>
0 1 1 1 1 1 0 5000 40. 0 0. 0. 0. 0. 0. 0. 0 2		<Parameters>
11		<Header - Five Axis>
<u>0. 0. 0</u>	<u>0.1142028 -0.9978952 6.2700608</u>	40. <u>12</u> <Coordinates>
(Probe center)	(Probe tip)	(vel.) (state_of_scan)
11		
-0.0048063 2.490622 0.3665092 0.1567081 1.6421697 6.6574981 40. <u>22</u>		
11		
	.	
	.	
	.	
11		
75.92571 75.70678 -0.24712 75.86059 76.7949 6.00859 40. <u>22</u>		
11		
75.94500 77.98028 -0.66548 75.95914 79.18902 5.56839 40. <u>32</u>		
1003		< Header - End of File >
0. 0. 0.		< Home Position coordinates>

Fig. 4-3: A Typical NCI File

4.2.1.1 NCI and Probe kinematics

It must be pointed out that the six coordinate positions described by the NCI file provides a complete description of a vector in \mathcal{R}^3 space. Further, the probe path generated is a five axis motion data. This latter fact implies that the set of all probe motion includes at most three translations along the three principal axis (X, Y, Z) and two rotations about any two of the principal axis. For example, a motion to reach a given target position might be composed of (say) 10mm along (an already defined) X axis, 4mm along Y axis, 7mm along the Z axis and 12° rotation about X axis and 8° rotation about Y-axis. Thus five parameters are to be known when ever a target position is to be reached from a given current position. Thus, the NCI specifies the (“current” and “target”) probe positions. A post processor determines the actual specific translations and rotations required to get from “current” to “target” position.

4.2.2 The Testbed Post Processor Module

The actual design and development of the post-processor is described in the next chapter, where a brief introduction to the theory of kinematics (forward and inverse) is also provided. The post processor as explained generates a translation and rotation parameter file. These parameters describe the probe and object motion. To test the validity of the probe and object motions that the post processor derives from the NCI file, a visualization program was utilized to actually see the path that the probe takes in going from the “current” to the “target” position. This visual aid helps in detecting motion accumulation errors, probe and object-surface interference during the motion. It actually confirms (visually) that the probe is indeed in the desired target position.

4.2.3 The Post Processor Motion Visualization Module

This simulation developed on a Silicon GraphicsTM serves as a feedback module that checks to see if the individual motions of the probe and object result in the probe correctly attaining its target position (as given in the NCI file). Since this module displays the motions generated, it conceptually gives rise to the decision block (shown in Fig. 4-2). It allows any possible errors to be flagged at this stage much before the actual motion is executed on the hardware, preventing any potential mishaps (probe or object surface damage).

4.2.4 The Interface Software

This is the software that executes the individual motions that comprise a scan and coordinates the data acquisition process. This module utilizes the post processor as its input. Conceptually it is shown in Fig. 4-2 in one module along with the hardware, as its design and functioning are tied with the modeling of the hardware.

In summary, the above discussion thus far, focused in a top-down model on the Eddy Current automation process, where we proceed from a bird's eye-view of the inspection process to examining each of the inspection modules in some detail. An introduction to the two main components of the scan automation process (section 4.2.3 and section 4.2.4) was provided. They are the main focus of the next chapter. The following chapter discusses probe kinematics problem and the design and implementation of the post processor module.

5. DEVELOPMENT OF THE TESTBED POST-PROCESSOR

The preceding chapters provided the background and motivation for this work. They discussed the definition of automation, established the need for automation and described the Eddy Current Inspection process. Stage VI as described, is the scan realization stage which is the experimental module in the inspection process. This chapter and the following chapter discuss the “motion automation” of the scanning system, that executes the scan (generated and simulated visually in stage II and confirmed again by simulation of the post processor module). The design and development of an “inverse kinematics algorithm” that is at the core of this automation project is presented after a brief introduction to kinematics theory.

5.1 Kinematics - Basic Theory

This section introduces the terminology and the background which are required to develop an abstract model of the physical hardware to realize the scans conceived in the CAM (NCI file).

5.1.1 Kinematics

Definition:

Kinematics: It is the science of motion which treats motion without regard to the forces that cause this motion. It deals with the study of position, velocity, acceleration and all higher order derivatives of the position variable(s). At the simplest level a complete description of the location of a body in three dimensional space requires the knowledge of two important factors: position, and orientation.

There are two fundamental problems in kinematics (as shown in Fig. 5-1).

- Direct kinematics or forward kinematics.
- Inverse kinematics.

In its simplest form, *forward kinematics* deals with the prediction of the final state of an entity (say a robot arm etc.), if certain motion operations like translation and rotation are performed on the entity.

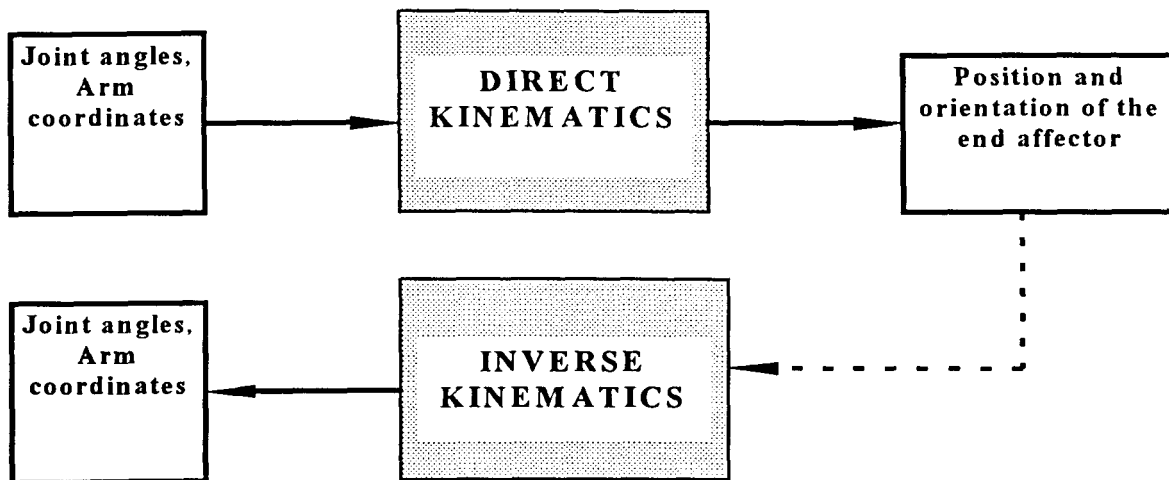


Fig. 5-1: Representation of direct and inverse kinematics

One of the most useful area where this technique finds application is in the area of *robot kinematics*. Here an arm may have multiple links. In that case, the final position is a function of the state of each of the individual links, i.e., since the links of a robot arm may rotate and/or translate with respect to a given reference frame, the total spatial displacement of the end-effector is due to the angular rotations and linear translations of the links. A 4x4 homogenous transformation matrix to describe the spatial relationship between two adjacent

rigid mechanical links is used⁶. We do not go further into this, as the technique of interest in solving our problem is the *inverse kinematics technique*; (for further reference on forward kinematics see [CRAIG] and [LEE]).

5.1.2 The Inverse Kinematics Problem

Problem statement: Given the position and orientation of the end-effector of the manipulator, calculate all possible sets of joint angles which could be used to attain this given position and orientation.

Inverse kinematics is not as straight forward as the forward kinematics. This is because, the equations that describe the problem are non-linear in nature, and often due to the second (or higher order) equations that describe the motion space multiple solutions present themselves. In the case of a complex (robot) arm with multiple links, there may not be an easy closed form solution. In case no solutions exists, then it implies that the manipulator may not attain the desired "target" position, i.e., the target is not present within the work area of the manipulator or end-effector. The presence of multiple solutions can also be explained by the fact that there simply exists more than one way to get from one position in a given 3D space.

To define and manipulate mathematical quantities which represent position and orientation we must first define a coordinate system and develop conventions for its representation. This is shown below.

⁶ This method by Denavit and Hartenberg [1955] reduces the direct kinematics problem to finding an equivalent homogenous matrix that relates the "hand coordinate frame" to a "reference coordinate frame"[CRAIG].

5.1.2.1 Reference Frames

Consider Fig. 5-2. The point P is described with respect to the frame $\{F\}$ ⁷. This description requires three quantities and is given by vector FP . Now the location of some point Q on this body is made with respect to P. Since P and Q are present on the same body, then Q is fixed with respect to P (thus despite any motion of the body w.r.t $\{F\}$, P will view Q as being stationary only). Because of this view of Q w.r.t P, it is convenient to represent the location of Q w.r.t P by a BODY-ATTACHED frame $\{B\}$. Thus, Q as seen from P is given by the vector PQ . Their vector description is now described. Let the frames, $\{F\}$ and $\{B\}$ be represented by the 3 principal unit vectors (f_1, f_2 and f_3) and (b_1, b_2 and b_3)

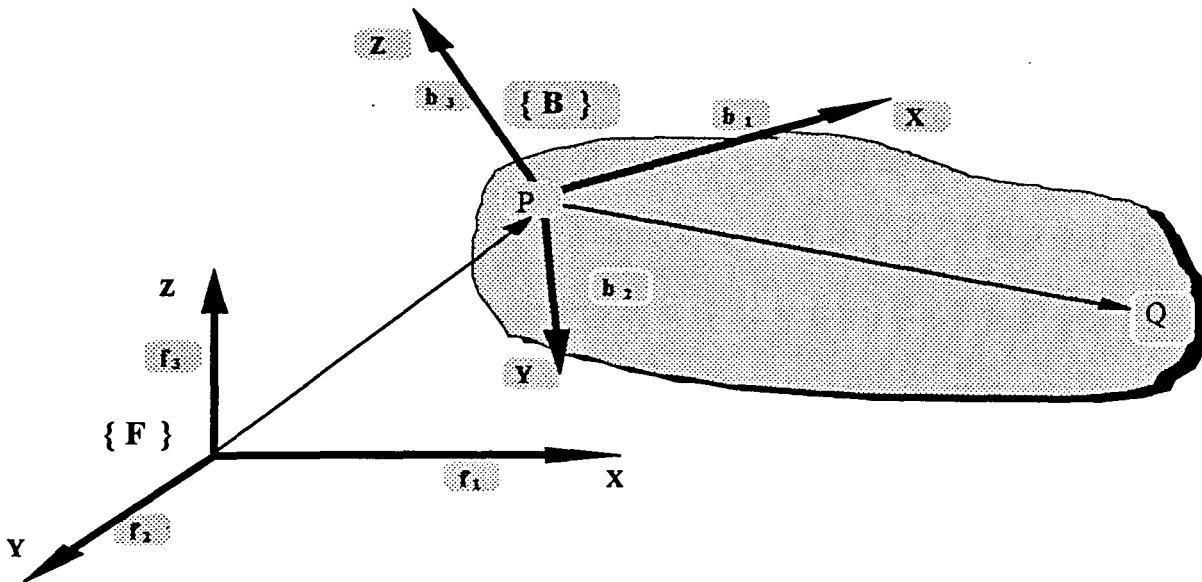


Fig. 5-2: Reference frames

⁷The format $\{X\}$, is used throughout this chapter to denote frames.

respectively. Then the point P is given by the vector ${}^F\mathbf{FP} = p_1\mathbf{f}_1 + p_2\mathbf{f}_2 + p_3\mathbf{f}_3$ and the vector PQ is given by ${}^B\mathbf{PQ} = q_1\mathbf{b}_1 + q_2\mathbf{b}_2 + q_3\mathbf{b}_3$. The quantities p_1, p_2 and p_3 and q_1, q_2 and q_3 are coefficients that represent the distance magnitude of the points (P and Q) from their respective frame origins⁸.

5.1.2.2 Position and Orientation

Now, position is usually a 3×1 vector. For e.g.: $\mathbf{FP} = \begin{bmatrix} p_1 \\ p_2 \\ p_3 \end{bmatrix}$ and $\mathbf{PQ} = \begin{bmatrix} b_1 \\ b_2 \\ b_3 \end{bmatrix}$. To

describe the body shown in Fig. 5-2 completely, we need not only the position but also its orientation. This is achieved by describing the BODY-ATTACHED frame {B} relative to frame {F} to get a complete description of the object. There are 3 principal vectors in frame {B} namely $\mathbf{b}_1, \mathbf{b}_2$ and \mathbf{b}_3 of unit magnitude. As seen from {F}, the tip (the arrow end in Fig. 5-2) of each of these three vectors can be expressed in terms of {F}. When written in the coordinate system of {F} the vectors are expressed as (3×1 vectors) $\mathbf{Fb}_1, \mathbf{Fb}_2, \mathbf{Fb}_3$. It is then convenient to stack up these vectors as the three columns of a 3×3 matrix expressed as,

$${}^F\text{ROT}_B = [\mathbf{Fb}_1 \quad \mathbf{Fb}_2 \quad \mathbf{Fb}_3] = \begin{bmatrix} r_{11} & r_{12} & r_{13} \\ r_{21} & r_{22} & r_{23} \\ r_{31} & r_{32} & r_{33} \end{bmatrix} \text{ (say).} \quad (5.1)$$

$$\Rightarrow \begin{bmatrix} f_1 \\ f_2 \\ f_3 \end{bmatrix} = \begin{bmatrix} r_{11} & r_{12} & r_{13} \\ r_{21} & r_{22} & r_{23} \\ r_{31} & r_{32} & r_{33} \end{bmatrix} \begin{bmatrix} b_1 \\ b_2 \\ b_3 \end{bmatrix} \Rightarrow \begin{bmatrix} r_{11} & r_{12} & r_{13} \\ r_{21} & r_{22} & r_{23} \\ r_{31} & r_{32} & r_{33} \end{bmatrix}^{-1} \begin{bmatrix} f_1 \\ f_2 \\ f_3 \end{bmatrix} = \begin{bmatrix} b_1 \\ b_2 \\ b_3 \end{bmatrix} \quad (5.2)$$

⁸ The superscripts F and B indicate the corresponding frames of reference

The matrix ${}^F\text{ROT}_B$ is called a *rotation matrix*. It represents the orientation information. In summary, *position* is represented by a vector and *orientation* by a matrix.

5.1.2.3 Transformations

It is often advantageous to describe the same quantity in terms of different frames of reference. This requires the use of *mappings* to change descriptions. Mappings involve, translated frames, rotated frames or a combination of the two. The mapping technique is illustrated with reference to Fig. 5-3. Consider the position of Q in Fig. 5-3. The location of Q w.r.t {F} is given by a vector \mathbf{FQ} . Now by vector addition,

$${}^F\mathbf{FQ} = {}^F\mathbf{FP} + {}^B\mathbf{PQ} \quad (5.3)$$

$$\text{Now, } {}^B\mathbf{PQ} = q_1\mathbf{b}_1 + q_2\mathbf{b}_2 + q_3\mathbf{b}_3 \quad (5.4)$$

thus, eqn.(5.2) becomes,

$${}^F\mathbf{FQ} = (p_1\mathbf{f}_1 + p_2\mathbf{f}_2 + p_3\mathbf{f}_3) + (q_1\mathbf{b}_1 + q_2\mathbf{b}_2 + q_3\mathbf{b}_3) \quad (5.5)$$

$$\text{Now, let } {}^F\mathbf{FQ} = x_1\mathbf{f}_1 + x_2\mathbf{f}_2 + x_3\mathbf{f}_3 \quad (5.6)$$

The determination of the unknown coefficients x_1 , x_2 , and x_3 is done by the following method using the *innerproduct*⁹ of two vectors. This yields the coefficients,

$$\begin{aligned} x_1 &= {}^F\mathbf{FQ} \cdot \mathbf{f}_1 = p_1 + q_1\mathbf{b}_1 \cdot \mathbf{f}_1 = p_1 + q_1|\mathbf{b}_1| \cdot |\mathbf{f}_1|\cos\theta_1 \\ x_2 &= {}^F\mathbf{FQ} \cdot \mathbf{f}_2 = p_2 + q_2\mathbf{b}_2 \cdot \mathbf{f}_2 = p_2 + q_2|\mathbf{b}_2| \cdot |\mathbf{f}_2|\cos\theta_2 \\ x_3 &= {}^F\mathbf{FQ} \cdot \mathbf{f}_3 = p_3 + q_3\mathbf{b}_3 \cdot \mathbf{f}_3 = p_3 + q_3|\mathbf{b}_3| \cdot |\mathbf{f}_3|\cos\theta_3 \end{aligned} \quad (5.7)$$

⁹ Innerproduct of two vectors A and B is given by $\mathbf{A} \cdot \mathbf{B} = |\mathbf{A}||\mathbf{B}|\cos\theta$, where θ represents the angle between the two vectors A and B.

The determination of the innerproducts $\mathbf{b}_x \cdot \mathbf{f}_x$ requires the orientation knowledge of $\{\mathbf{B}\}$ w.r.t $\{\mathbf{F}\}$. This knowledge is also present in the rotation matrix shown in eqns. (5.1) and (5.2) and can be used to determine the coefficients, x_1 , x_2 , and x_3 . This latter technique is equivalent to the above technique but allows a more compact way of expressing the above steps. This is shown below.

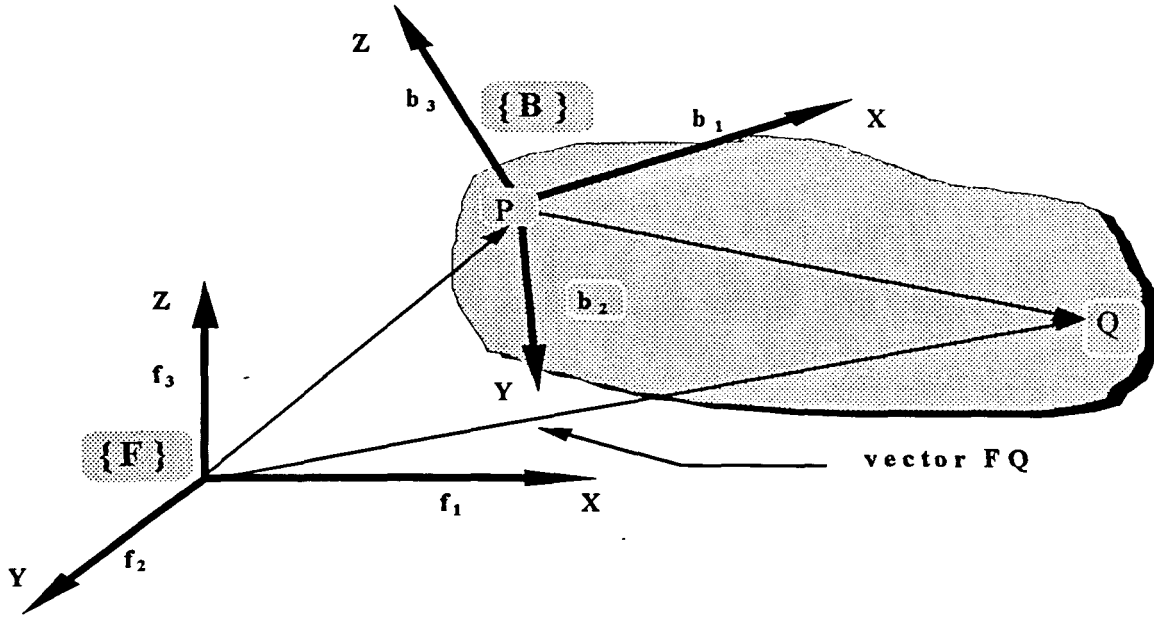


Fig. 5-3: Transforming the frame description

The equation, ${}^F\mathbf{FQ} = {}^F\mathbf{FP} + {}^B\mathbf{PQ}$ consists of two quantities expressed w.r.t two different frames. To be actually summed up it must be expressed in terms of one frame of reference, so that the corresponding quantities can then be summed. This is done by using (5.2) and expressing ${}^B\mathbf{PQ}$ solely in terms of $\{\mathbf{F}\}$ (shown as ${}^F\mathbf{PQ}$). Thus,

$${}^F\mathbf{PQ} = {}^F\text{ROT}_B {}^B\mathbf{PQ}$$

$$\begin{aligned}
\Rightarrow {}^B\mathbf{PQ} &= [{}^F\text{ROT}_B]^{-1} {}^F\mathbf{PQ} \\
\Rightarrow {}^F\mathbf{FQ} &= {}^F\mathbf{FP} + ({}^F\text{ROT}_B {}^B\mathbf{PQ}) \\
\Rightarrow \begin{bmatrix} x_1 \\ x_2 \\ x_3 \end{bmatrix} &= \begin{bmatrix} p_1 \\ p_2 \\ p_3 \end{bmatrix} + \begin{bmatrix} r_{11} & r_{12} & r_{13} \\ r_{21} & r_{22} & r_{23} \\ r_{31} & r_{32} & r_{33} \end{bmatrix}^{-1} \begin{bmatrix} q_1 \\ q_2 \\ q_3 \end{bmatrix} \quad (5.8)
\end{aligned}$$

5.1.2.4 Basic Concepts of Motion in Space

For mathematical understanding, motion is divided into two components, namely, (1) *translation* and (2) *rotation*.

To go from a given position, (called here, the “*current*” position) to a desired position, (called here, the “*target*” position) we need to use a combination of the above two motions. The exact type of motion actually employed is dependent on the positions and the freedom of degrees available to the given object undergoing the motion. Given the “*current*” and “*target*” positions, the science of determining quantitatively the exact motion components is called “*Inverse kinematics*”. As mentioned previously multiple solutions or no solutions may exist. Some important properties of motion are highlighted below: All the below properties apply to motion in 3D space too.

- Translation is commutative. This implies that the order of motions does not matter. If *x-axis* motion is followed by *y-axis* motion, then the final position reached is the same even if the order is reversed.
- Rotation is *not commutative*. This implies that if an entity rotates, first along the *x-axis* followed by a rotation along the *y-axis*, then the position reached may not be

the same if the order is reversed. This is seen by the fact that rotation is represented by a matrix and matrix multiplication is not always commutative.

- Given a translation motion component and then a rotation motion component, the two are commutative. This implies that an entity may translate and rotate or vice-versa.

5.2 Symbols And Notations

The previous section described the basic concepts of kinematics that lay the ground for the development of the post processor algorithm. This chapter summarizes the symbols and notations introduced earlier and to be used in the succeeding section.

- Vectors are represented in **bold and uppercase letters**. Only the unit vectors are however represented in bold and lower case; ; e.g., **PQ**, **e₁**, **e₂** etc.
- Reference frames are represented by the notation {REFERENCE FRAME}; e.g., a frame A is represented as {A}. The origin of any {A}, is denoted by A.
- The notation ^A**P** implies that the vector **P** is described with respect to {A}. Alternatively, the equivalent notation **AP** is also used; in the latter case the reference is implicit. Here, A refers to the origin of {A}.
- Scalars quantities are not in bold case and may be shown in lower case or upper case; e.g., p, q, CC, CT etc.
- The subscripts 1, 2 and 3 represent the coefficients of the vector along the three axis x, y and z respectively; e.g., p₁, p₂ and p₃ belong to the x, y and z axis..

- The rotation matrices are denoted by either “ROT” or by the compact notation

$$\sum_{\beta=1,2,3} (angle).$$

- The variables representing the target state have a prime (') attached to them to distinguish them from other variables

5.3 Design of the Motion Automation Algorithm

Overview: The post processor is a software module that contains the actual motion components that constitute an entire scan (generated in the CAM and contained in the NCI file). As was explained earlier, the hardware needs to be given the basic individual motion segments and hence the post processor serves as a communication layer (between the software scan generation stage and the hardware realization stage) that contains within it a knowledge of the hardware and also an understanding of the NCI data. The design of the motion automation algorithm is the design of a post processor for the given hardware.

This section proceeds with the design, by first describing the intuitive idea behind the algorithm and then proceeding to present a formal mathematical model of the algorithm. The next chapter describes the software implementation of the mathematical model in abstract terms.

5.3.1 A method to Enhance the Scanning Capability

A smaller representation of the hardware schematic (shown in chap. 3) is again shown in Fig. 5-4. Now, the scans conducted before the development of this algorithm were limited

to scanning in a flat plane over a given surface and to scanning over a given part of a circular object, particularly the pin (the object geometry is shown in chapter 7). The motion control programs developed to conduct such scans took advantage of the object geometry simplicity and presence of any symmetry [Bugaru A].

These programs as is evident, could not be reused and thus each time a new object needs to be scanned a new program must be written to address the needs of scanning that particular geometry. Further, in the case of complicated geometries, this is a non-trivial task with lot of developmental time overhead. Also as can be seen in Fig. 5-4, the probe can rotate only about one axis (the x-axis).

This imposes the limitation that the probe can conduct only such scans that do *not* require the probe to rotate about two principal axis (say x-axis and y-axis in Fig. 5-4). But, it can be seen that although the probe cannot rotate about the y-axis, the object or sample to be scanned can rotate about the y-axis. This presents an interesting opportunity whereby the object is rotated to *compensate* for the probe's lack of freedom of rotation.

The above fact implies that it is possible to enhance the utility of the hardware so that the hardware can now execute scans that are more complicated than simple flat scans or scans requiring probe rotation along only one axis. This allows the hardware to utilize more than 4 axis (three translation and one rotation axis) so that effectively, it can place the probe on the object, as per the position given by the NCI file. Thus scans utilizing 5-axis of motion, generated on the CAM, can be executed on the hardware.

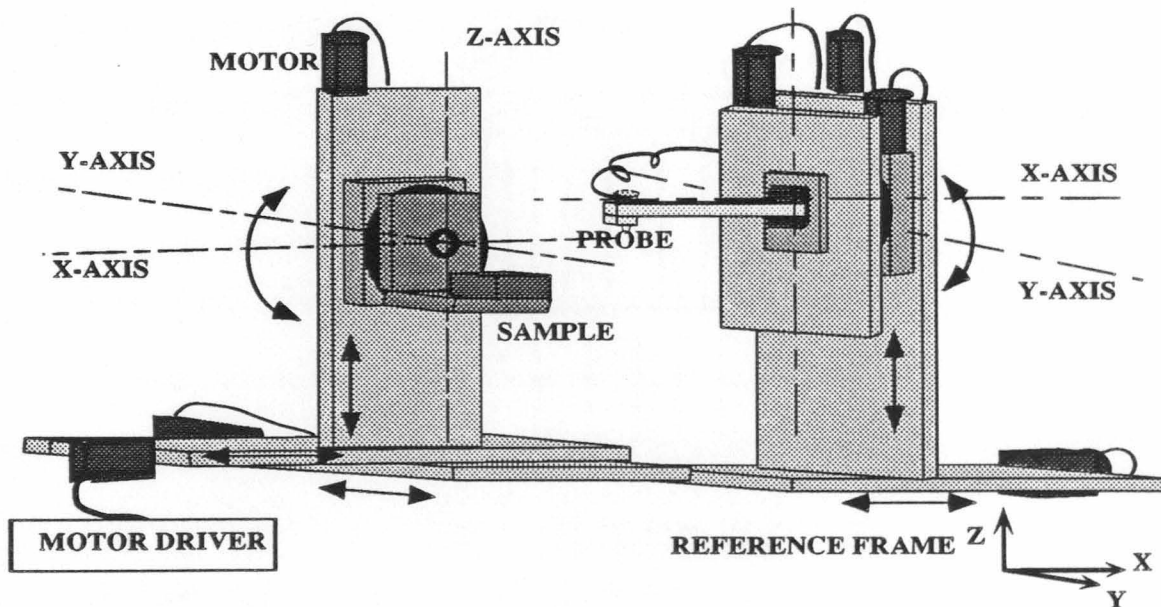


Fig. 5-4: Hardware schematic representation

Now, an algorithm that determines the translation and rotations required of the probe¹⁰, and transfers to the object all motions that cannot be realized by the probe, (due to lack of freedom of motion) provides in general,

- a means to enhance the scanning capability of the hardware by utilizing the freedom of motion of the object
- a way to break down any complex scan into its constituent motion components.

This allows different types of scans to be automatically executed on the hardware, thus automating the scanning process and reducing or eliminating any object specific motion control in the software.

¹⁰ In order to go from "current" to "target" position or from some n th step to $n+1$ th step.

5.3.2 Motion from n th to $n+1$ th Step

The below subsection explains the conceptual idea behind the algorithm design by means of two simple examples.

5.3.2.1 Simple Probe Motion and Object Motion

Consider a motion from step n th to $n+1$ th step, as shown in Fig. 5-5. Here, to get from step n th to step $n+1$ th, the probe undergoes translation, which moves its “center” from “current”(CR) to “target”(TR) position. At the position “TR” it undergoes rotations about the x -axis and the y -axis and its “tip” is then aligned along with the target position. In Fig. 5-5 the probe undergoes two rotations (P_x and P_y) to align with the desired position. At this position the probe is perpendicular to the object surface at that point.

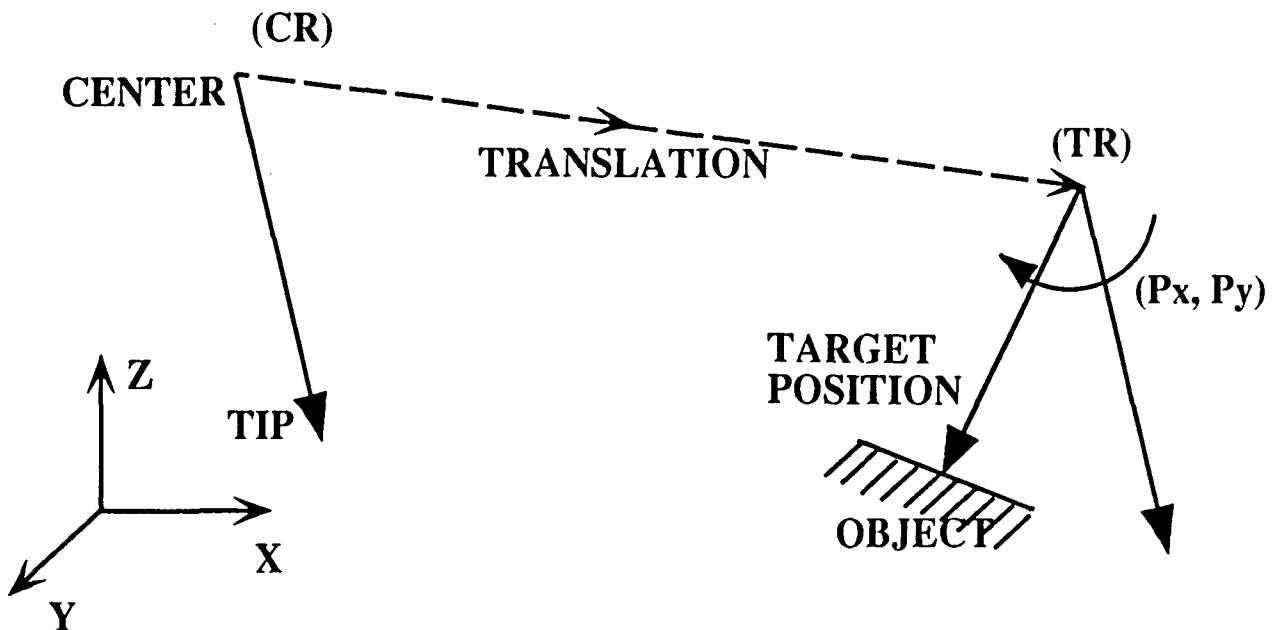


Fig. 5-5: Motion from n th to $n+1$ th step.

The concept of object rotations is explained below with reference to 2D (\mathbb{R}^2) space. Here, in this example, the probe is restricted from rotating and the object is made to rotate (to get the target position on the object) to the probe. This principle applies in 3D space too. In Fig. 5-6 the probe center is *translated* to the desired position., but the object is *rotated* and *translated* to the position of the probe tip (the position “INTR”). Notice that the object in Fig. 5-6 must rotate by the same angle (in magnitude, but not necessarily in direction) as the probe would have, if allowed. However the object’s rotation about the point “O” resulted in the desired position not being directly under the tip of the probe. Hence, to compensate, the object needed to be translated too to get the desired position under the probe tip. This example illustrates that if the object rotates, translation too varies. This condition is illustrated mathematically in the algorithm design.

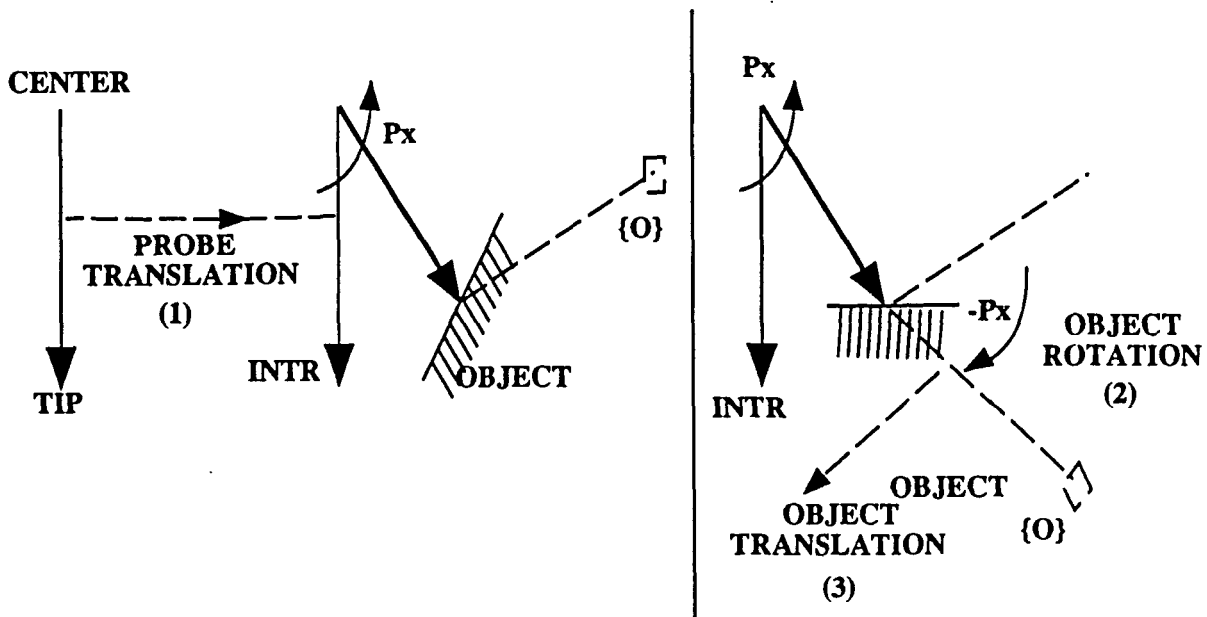


Fig. 5-6: Probe and object motions

5.3.2.2 Algorithm Design

This section describes the modeling of the scanning hardware. There exists three laboratory frames with respect to which all motion is referenced. There are two entities called the “probe” and the “object” (the scanned object). The three reference frames are,

- (1) A fixed frame {F}, serving as the universal frame. This is the laboratory frame. It has three mutually perpendicular unit vectors given by ${}^F\mathbf{e}_1$, ${}^F\mathbf{e}_2$, and ${}^F\mathbf{e}_3$ lying along the three principal directions X, Y and Z respectively. These directions lie parallel to the motion of the hardware axis show in Fig. 5-4.
- (2) A probe attached frame {C}. This is a body attached frame. Its unit vectors in the three principal directions are given by ${}^P\mathbf{e}_1$, ${}^P\mathbf{e}_2$ and ${}^P\mathbf{e}_3$. The probe rotates about its X axis (vector ${}^P\mathbf{e}_1$). Also, ${}^P\mathbf{e}_1 \parallel {}^F\mathbf{e}_1$ and this relationship is invariant through the scan. The probe frame {C} is thus conceptually obtained from the lab. frame {F} by the translation vector FC and the rotation φ around ${}^F\mathbf{e}_1$. Thus we represent the relationship between the probe frame and the fixed frame mathematically as, $\{{}^P\mathbf{e}_\alpha\}$

$$= \sum_{\beta} \Phi_{\beta} {}^F\mathbf{e}_{\beta} \quad \forall \alpha, \beta = 1,2,3 \text{ and } [\Phi]_{\alpha} = \begin{bmatrix} 1 & 0 & 0 \\ 0 & \cos \varphi & -\sin \varphi \\ 0 & \sin \varphi & \cos \varphi \end{bmatrix}. \text{ This is the}$$

rotation matrix for rotations about the X axis.

- (3) An object attached frame {O}. This is a body attached frame. Its unit vectors in the three principal directions are given by ${}^O\mathbf{e}_1$, ${}^O\mathbf{e}_2$ and ${}^O\mathbf{e}_3$. The object rotates about its Y-axis (vector ${}^O\mathbf{e}_1$). Also, ${}^O\mathbf{e}_2 \parallel {}^F\mathbf{e}_2$ and this relationship is invariant. The Object frame {O} is obtained conceptually from the lab. frame {F} by the

translation vector FO and the rotation θ about ${}^{\circ}e_2$. This is represented mathematically by, $\{{}^{\circ}e_{\alpha}\} = \sum_{\beta} \Theta_{\beta} {}^{\circ}e_{\beta}$, $\forall \alpha, \beta = 1,2,3$ and $[\Theta]_{\alpha} =$

$$\begin{bmatrix} \cos\theta & 0 & \sin\theta \\ 0 & 1 & 0 \\ -\sin\theta & 0 & \cos\theta \end{bmatrix}. \text{ This matrix is the rotation matrix for rotation by } \theta \text{ about the}$$

Y-axis. We introduce the constraint that the object frame, $\{O\}$ does not explicitly translate. Its translation, if required, is transferred to the probe frame $\{C\}$. The above implies, $FO = FO'$.

The superscripts represent the type of frame, while the subscripts 1, 2 and 3 represent the X, Y and Z axis respectively. Fig. 5-7 shows the frame relationships, and the initial location of the entities (probe and object). We now proceed to describe the design of the algorithm.

GIVEN:

1. The initial position of the probe in the probe frame (at $t = 0$, position = #1) is given by, $CT = -L {}^p e_3$, where L is the length of the probe (known).
2. Also, from the NCI file we know the current (step n) and target (step $n+1$ th) positions of the probe tip and center (six coordinates describe a vector in space). These positions are the positions of the probe as viewed by the object, and hence they are described with respect to $\{O\}$, i.e., ${}^{\circ}e_{\alpha} \forall \alpha = 1,2,3$.

The current position of the center (OC) and tip (OT) are given by,

$$OC = \sum_{\alpha} c_{\alpha} {}^{\circ}e_{\alpha} = c_1 {}^{\circ}e_1 + c_2 {}^{\circ}e_2 + c_3 {}^{\circ}e_3. \text{ and,}$$

$$\mathbf{OT} = \sum_{\alpha} t_{\alpha} {}^{\circ}\mathbf{e}_{\alpha} = t_1 {}^{\circ}\mathbf{e}_1 + t_2 {}^{\circ}\mathbf{e}_2 + t_3 {}^{\circ}\mathbf{e}_3.$$

The target position to be attained (position $n+1$) by the probe center and tip are given by,

$$\mathbf{O'C'} = \mathbf{OC'} = \sum_{\alpha} cc_{\alpha} {}^{\circ}\mathbf{e}_{\alpha} = cc_1 {}^{\circ}\mathbf{e}_1 + cc_2 {}^{\circ}\mathbf{e}_2 + cc_3 {}^{\circ}\mathbf{e}_3 \text{ and}$$

$$\mathbf{O'T'} = \mathbf{OT'} = \sum_{\alpha} tt_{\alpha} {}^{\circ}\mathbf{e}_{\alpha} = tt_1 {}^{\circ}\mathbf{e}_1 + tt_2 {}^{\circ}\mathbf{e}_2 + tt_3 {}^{\circ}\mathbf{e}_3.$$

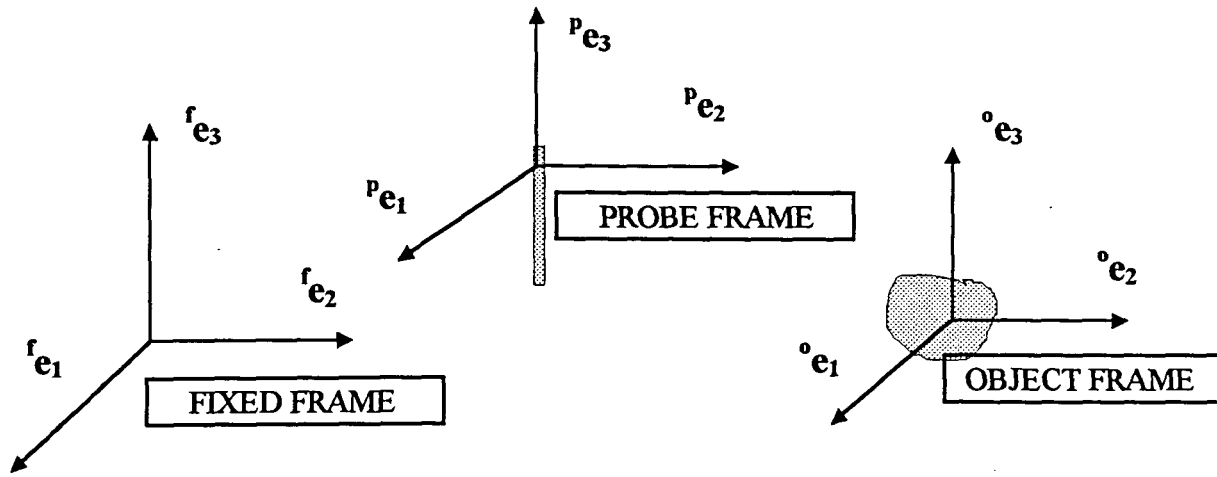


Fig. 5-7: Frame relationships

OBJECTIVE:

We now define the components of a motion (from n th to $n+1$ th step). The probe needs to move from \mathbf{CT} to some $\mathbf{C'T'}$. Conceptually this motion consists of,

1. Translation from \mathbf{C} to $\mathbf{C'}$. Let this be given by (say) \mathbf{S} .
2. Rotation about the fixed X and/or Y-axis so that \mathbf{T} lies after the motion in the position given by $\mathbf{T'}$. The object too can rotate. However, for the sake of

simplifying the calculations and reducing actual motion time, we inhibit the object's translation.

3. The (possible) rotations of the object and the probe however will change the orientations of {C} and {O} w.r.t {F}.

The above conditions result in the motion being represented by the equations below:

1. $\mathbf{FC}' = \mathbf{FC} + \mathbf{S}$. (5.9)
2. $\mathbf{FO}' = \mathbf{FO}$
3. $\{^c\mathbf{e}_\alpha\} = \sum_{\beta} \Delta\Phi_{\beta} {}^f\mathbf{e}_{\beta}$ and $\{^o\mathbf{e}_\alpha\} = \sum_{\beta} \Delta\Theta_{\beta} {}^f\mathbf{e}_{\beta} \quad \forall \alpha, \beta = 1,2,3$. $\Delta\varphi$ and $\Delta\theta$ represent the

incremental change in orientation (of {C} and {O} w.r.t {F}) in moving from n to $n+1$ th position.

The above equations represent the current state and the six parameters (three translations and two rotations) needed to reach the next state. These parameters are as yet unknown and we represent them (as above) by \mathbf{S} , $\Delta\varphi$ and $\Delta\theta$. Our objective thus is the determination of these three unknowns.

DETERMINATION OF $\Delta\varphi$ AND $\Delta\theta$:

In the n th step, let the orientation of the probe w.r.t the fixed frame be given by some φ and let the orientation of the object w.r.t the fixed frame be some θ . After the motion (in the $n+1$ th position) let these quantities be φ' and θ' . Now, the relationship between CT and C'T' can be expressed as,

$$\mathbf{CT} = -L {}^p\mathbf{e}_3 = -L \sum_{\beta} [\Phi_{\beta}]^3 {}^f\mathbf{e}_{\beta} \text{ and}$$

$$\begin{aligned} \mathbf{C}'\mathbf{T}' &= -\mathbf{L}^p \mathbf{e}'_3 = -\mathbf{L} \sum_{\beta} [\Phi'_{\beta}]^3 \mathbf{e}_{\beta} = -\mathbf{L} \sum_{\beta} (\Delta\Phi)_{\beta} \Phi \mathbf{e}_{\beta} = \sum_{\beta} (\Delta\Phi)_{\beta} (-\mathbf{L} \Phi \mathbf{e}_{\beta}). \\ \Rightarrow \mathbf{C}'\mathbf{T}' &= \sum_{\beta} (\Delta\Phi)_{\beta} (\mathbf{C}\mathbf{T}) \end{aligned} \quad (5.10)$$

Also, $\mathbf{C}\mathbf{T}$ and $\mathbf{C}'\mathbf{T}'$ are related as shown below:

$$\mathbf{C}\mathbf{T} = \mathbf{O}\mathbf{T} - \mathbf{O}\mathbf{C} = \sum_{\alpha} (t_{\alpha} - c_{\alpha}) \mathbf{e}_{\alpha} = \sum_{\alpha\beta} (t_{\alpha} - c_{\alpha}) (\Theta_{\beta} \mathbf{e}_{\beta}) \quad (5.11)$$

$$\mathbf{C}'\mathbf{T}' = \mathbf{O}'\mathbf{T}' - \mathbf{O}'\mathbf{C}' = \mathbf{O}\mathbf{T}' - \mathbf{O}\mathbf{C}'$$

$$\Rightarrow \mathbf{C}'\mathbf{T}' = \sum_{\alpha} (tt_{\alpha} - cc_{\alpha}) \mathbf{e}'_{\alpha} = \sum_{\alpha\beta} (tt_{\alpha} - cc_{\alpha}) (\Theta'_{\beta} \mathbf{e}_{\beta}) \quad (5.12)$$

From, (5.10) and (5.12), equating the two expressions of $\mathbf{C}'\mathbf{T}'$, we have,

$$\begin{aligned} \sum_{\beta} (\Delta\Phi)_{\beta} (\mathbf{C}\mathbf{T}) &= \sum_{\alpha\beta} (tt_{\alpha} - cc_{\alpha}) (\Theta'_{\beta} \mathbf{e}_{\beta}). \\ \Rightarrow \sum_{\beta} (\Delta\Phi)_{\beta} (t_{\alpha} - c_{\alpha}) (\Theta_{\beta} \mathbf{e}_{\beta}) &= \sum_{\alpha\beta} (tt_{\alpha} - cc_{\alpha}) (\Theta'_{\beta} \mathbf{e}_{\beta}). \end{aligned} \quad (5.13)$$

Neglecting the unit vectors of $\{\mathbf{F}\}$, we write (5.13) as,

$$\sum_{\beta} (\Delta\Phi)_{\beta} (\Theta_{\beta}) (t_{\alpha} - c_{\alpha}) = \sum_{\alpha\beta} (\Theta'_{\beta}) (tt_{\alpha} - cc_{\alpha}) \quad (5.14)$$

Note that in the above equations, $\Delta\Phi$ and Θ'_{β} are the rotation matrices and are not to be confused with the angles $\Delta\phi$ and θ' . Also, the running indices α and β range from 1 to 3.

Now, (5.14) may be expressed in matrix notation as,

$$\begin{bmatrix} 1 & \cos \Delta\phi & -\sin \Delta\phi \\ \sin \Delta\phi & \cos \Delta\phi & 1 \end{bmatrix} \begin{bmatrix} \cos \theta & \sin \theta \\ -\sin \theta & \cos \theta \end{bmatrix} \begin{bmatrix} t_1 - c_1 \\ t_2 - c_2 \\ t_3 - c_3 \end{bmatrix} = \begin{bmatrix} \cos \theta' & \sin \theta' \\ -\sin \theta' & \cos \theta' \end{bmatrix} \begin{bmatrix} tt_1 - cc_1 \\ tt_2 - cc_2 \\ tt_3 - cc_3 \end{bmatrix} \quad (5.15)$$

Now,

$$\begin{bmatrix} \cos \theta' & \sin \theta' \\ -\sin \theta' & \cos \theta' \end{bmatrix} = \begin{bmatrix} \cos \Delta \theta & \sin \Delta \theta \\ -\sin \Delta \theta & \cos \Delta \theta \end{bmatrix} \begin{bmatrix} \cos \theta & \sin \theta \\ -\sin \theta & \cos \theta \end{bmatrix} \quad (5.16)$$

and let,

$$\begin{bmatrix} \xi_1 \\ \xi_2 \\ \xi_3 \end{bmatrix} = \begin{bmatrix} \cos \theta & \sin \theta \\ -\sin \theta & \cos \theta \end{bmatrix} \begin{bmatrix} t_1 - c_1 \\ t_2 - c_2 \\ t_3 - c_3 \end{bmatrix} \text{ and } \begin{bmatrix} \eta_1 \\ \eta_2 \\ \eta_3 \end{bmatrix} = \begin{bmatrix} \cos \theta & \sin \theta \\ -\sin \theta & \cos \theta \end{bmatrix} \begin{bmatrix} tt_1 - cc_1 \\ tt_2 - cc_2 \\ tt_3 - cc_3 \end{bmatrix}.$$

$$\Rightarrow \begin{bmatrix} 1 & \cos \Delta \varphi & -\sin \Delta \varphi \\ \sin \Delta \varphi & \cos \Delta \varphi \end{bmatrix} \begin{bmatrix} \xi_1 \\ \xi_2 \\ \xi_3 \end{bmatrix} = \begin{bmatrix} \cos \Delta \theta & \sin \Delta \theta \\ -\sin \Delta \theta & \cos \Delta \theta \end{bmatrix} \begin{bmatrix} \eta_1 \\ \eta_2 \\ \eta_3 \end{bmatrix} \quad (5.17)$$

The above matrix can now be solved for $\Delta \theta$ and $\Delta \varphi$. As expected, there is more than one solution¹¹ for the unknowns. The equations to solve for the unknowns are, $\xi_1 = \cos \Delta \theta \eta_1 + \sin \Delta \theta \eta_3$ and $\eta_2 = \cos \Delta \varphi \xi_2 - \sin \Delta \varphi \xi_3$. These equations may be solved using standard techniques to solve trigonometric equations.

Due to the presence of multiple solutions, the selection of the correct solution pair of $\Delta \theta$ and $\Delta \varphi$ is important. This selection can be made by ensuring that the solution satisfies the condition, $\{\eta^\alpha\} \rightarrow \{\xi^\alpha\}$.

Thus, we now know the angle of rotation of the object ($\Delta \theta$) and the probe ($\Delta \varphi$). The translation vector S is next determined. Note that the determination of translation requires a knowledge of the object's current orientation ($\Delta \theta$) determined above.

¹¹ because, \exists three equations and two unknowns

DETERMINATION OF THE TRANSLATION COMPONENT:

The translation to be provided to the probe is denoted by the vector S . As mentioned earlier, there are two factors that go into the determination of the final translation (S). These are, (1) the translation by the probe center (C) from the current position to the target position. and (2) the translation by the object. This latter translation is (inherently) present whenever the object rotates (i.e., $\Delta\theta \neq 0$) and when the object is not symmetric in geometry about its center of rotation. The effect of this translation is to bring the point to be scanned (the target position) directly underneath the current position of the probe. The derivation of an expression for the translation is shown below:

$$\text{Now, } \mathbf{FC}' = \mathbf{FC} + \mathbf{S}$$

$$\Rightarrow \mathbf{FO}' + \mathbf{O'C}' = \mathbf{FO} + \mathbf{OC} + \mathbf{S}$$

$$\Rightarrow \mathbf{S} = \mathbf{O'C}' - \mathbf{OC} \quad (\text{since, } \mathbf{FO}' = \mathbf{FO})^{12}$$

$$\Rightarrow \mathbf{S} = \sum_{\alpha} c c_{\alpha}' \mathbf{e}_{\alpha} - \sum_{\alpha} c_{\alpha} \mathbf{e}_{\alpha} \quad (5.18)$$

The above equation describes the translation vector in terms of the object frame $\{O\}$. Now, the actual physical translating units (the motors) are fixed and their orientation with respect to $\{F\}$ remains always the same throughout the scan, irrespective of the orientation of the probe and/or the object. Hence, we need to express the translation S with respect to (w.r.t) the fixed frame $\{F\}$.

¹² $\mathbf{FO}' = \mathbf{FO}$, since we explicitly constrained the object from translating and instead transferred the translation that is to be undergone by the object to the probe. (see 5.3.2.2)

Now, the unit vectors, $\{^o\mathbf{e}_\alpha\}_{\alpha=1,2,3}$ have an orientation of $\theta' (= \theta + \Delta\theta)$ w.r.t the unit vectors, $\{^f\mathbf{e}_\alpha\}_{\alpha=1,2,3}$ of the fixed frame and the vectors $\{^o\mathbf{e}_\alpha\}_{\alpha=1,2,3}$ have a orientation of θ w.r.t the unit vectors of the fixed frame $\{F\}$. We thus need to express equation (5.18) w.r.t the fixed frame. Thus, expressing (5.18) w.r.t the fixed frame we have,

$$\mathbf{S} = \sum_{\alpha} cc_{\alpha} \left(\sum_{\beta} \Theta_{\alpha}^{\prime\beta} {}^f\mathbf{e}_{\alpha} \right) - \sum_{\alpha} c_{\alpha} \left(\sum_{\beta} \Theta_{\alpha}^{\beta} {}^f\mathbf{e}_{\alpha} \right)$$

$$\text{since, } [\Theta_{\alpha}^{\prime\beta}] = [\Theta_{\alpha}^{\beta}] [\Delta\Theta_{\alpha}^{\beta}] = [\Delta\Theta_{\alpha}^{\beta}] [\Theta_{\alpha}^{\beta}] \quad (\text{from 5.16})$$

$$\Rightarrow \mathbf{S} = \sum_{\beta} \Theta_{\alpha}^{\beta} \left\{ \sum_{\gamma} (\Delta\Theta)_{\alpha}^{\gamma} cc_{\gamma} {}^f\mathbf{e}_{\alpha} - c_{\beta} {}^f\mathbf{e}_{\alpha} \right\}$$

$$\text{or } ({}^f\mathbf{e}_{\alpha}, \mathbf{S}) = \sum_{\beta} \Theta_{\alpha}^{\beta} \left\{ \sum_{\gamma} (\Delta\Theta)_{\alpha}^{\gamma} cc_{\gamma} - c_{\beta} \right\} \quad (5.19)$$

If, $\mathbf{S} = s_1 {}^f\mathbf{e}_1 + s_2 {}^f\mathbf{e}_2 + s_3 {}^f\mathbf{e}_3$ (say)

In matrix form, (5.19) is,

$$\begin{bmatrix} s_1 \\ s_2 \\ s_3 \end{bmatrix} = \begin{bmatrix} \cos \theta & \sin \theta \\ & 1 \\ -\sin \theta & \cos \theta \end{bmatrix} \left\{ \begin{bmatrix} \cos \Delta \theta & \sin \Delta \theta \\ & 1 \\ -\sin \Delta \theta & \cos \Delta \theta \end{bmatrix} \begin{bmatrix} cc_1 \\ cc_2 \\ cc_3 \end{bmatrix} - \begin{bmatrix} c_1 \\ c_2 \\ c_3 \end{bmatrix} \right\} \quad (5.20)$$

The above expression in the matrix form gives the translation components, s_1 , s_2 , and s_3 (coefficients) of the vector \mathbf{S} in the three principal directions, X, Y and Z of the fixed frame, $\{F\}$ respectively.

We have now derived a closed form expression for the rotations θ and φ of the probe and object respectively and the translation to be undergone by the probe, given by the translation vector \mathbf{S} . The equations describing the rotations and the translation are summarized below.

The equations to determine rotations are (from 5.17):

$$1. \begin{bmatrix} 1 & & \\ & \cos \Delta \varphi & -\sin \Delta \varphi \\ & \sin \Delta \varphi & \cos \Delta \varphi \end{bmatrix} \begin{bmatrix} \xi_1 \\ \xi_2 \\ \xi_3 \end{bmatrix} = \begin{bmatrix} \cos \Delta \theta & \sin \Delta \theta & \\ & 1 & \\ -\sin \Delta \theta & \cos \Delta \theta & \end{bmatrix} \begin{bmatrix} \eta_1 \\ \eta_2 \\ \eta_3 \end{bmatrix} \quad (5.21)$$

The equations to determine the translation are (from 5.19):

$$\begin{bmatrix} s_1 \\ s_2 \\ s_3 \end{bmatrix} = \begin{bmatrix} \cos \theta & \sin \theta \\ & 1 \\ -\sin \theta & \cos \theta \end{bmatrix} \left\{ \begin{bmatrix} \cos \Delta \theta & \sin \Delta \theta \\ & 1 \\ -\sin \Delta \theta & \cos \Delta \theta \end{bmatrix} \begin{bmatrix} cc_1 \\ cc_2 \\ cc_3 \end{bmatrix} - \begin{bmatrix} c_1 \\ c_2 \\ c_3 \end{bmatrix} \right\} \quad (5.22)$$

The post processor reads in two consecutive pairs of NCI data (the current and the target positions), applies the above algorithm and determines the five parameters, namely $\Delta \theta$, $\Delta \varphi$, s_1 , s_2 , and s_3 . A new set of parameters is thus created, which are used directly by the hardware interface program to position the hardware.

5.4 Solution Characteristics

The characteristics of the solution derived are

- There is no order dependency between θ and φ . Hence in the actual scan execution, the object and the probe may be operated in any order. This also contains the potential to execute the object and probe motions in parallel and thus cut down the motion segment time.
- The order of the operations, (translation and the set of rotations) can be interchanged.

- The solution derivation as shown above assumes that the object rotates about the Y-axis and the probe rotates about the X-axis. This is not a rigid requirement and can be changed. We however, assign the axis about which the object rotates (in the hardware) as the Y-axis and the probe rotation axis as the X-axis. A right hand rule is used to establish the direction of the unit vectors of the frames.
- To avoid accumulation errors (due to calculation truncations) which occur in actual calculations, we use $\mathbf{OC}_{\text{Calculated}}$ and $\mathbf{OT}_{\text{Calculated}}$ of stage n as the \mathbf{OC} and \mathbf{OT} for stage $n+1$. Conceptually,

$$(\mathbf{OC}_{\text{Calculated}}, \mathbf{OT}_{\text{Calculated}})_{n+1} = (\mathbf{OC}, \mathbf{OT})_n + (\Delta\theta, \Delta\phi, \mathbf{S})_n .$$

Ideally we would like $(\mathbf{OC}_{\text{Calculated}}, \mathbf{OT}_{\text{Calculated}})_{n+1} = (\mathbf{OC}', \mathbf{OT}')_n$.

6. ALGORITHM TESTING AND SCAN RESULTS

6.1 Experimental Evaluation Of The Motion Algorithm

The goal of developing a scanning system that does not include any object geometry specific features, was tested by designing two test pieces with curved surfaces. The following section describes the test pieces and the scans.

6.1.1 Test Parts-Description

Two test pieces(aluminum blocks) were manufactured with one block having a uni-directional curvature and the other having a bi-directional curvature (Block-1 and Block-2, as shown in Fig. 6-1 and Fig. 6-2) On each of these blocks 3 sets of EDM notches were created. The dimensions of the notches were 40x5 mils, 20x5 mils and 10x5 mils. The detection of these notches on the complex surfaces would serve as a good test for the automation system.

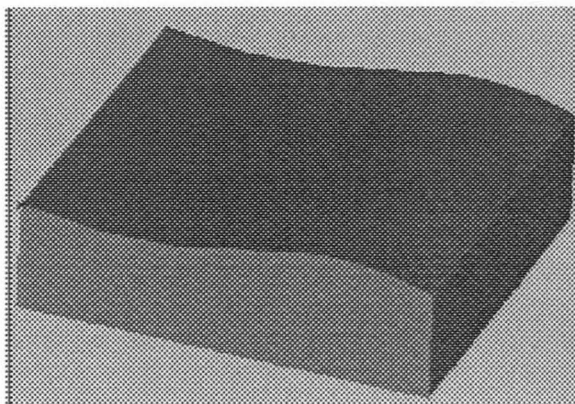


Fig. 6-1: Single curvature (Block1)

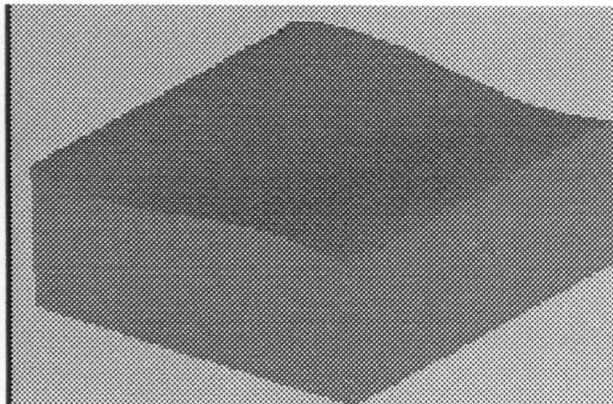


Fig. 6-2: Double curvature (Block2)

6.1.2 Types of Scan

To test the scanning system three types of scans were conducted on the two blocks. The results obtained from these three different scans clearly highlight the sensitivity of the measurements to the perpendicularity of the probe. The three types of scans are here classified as, Flat, no-tilt and Full scans. Each of these scan procedures is described below (Fig. 6-3).

- **Flat scan**

In the flat scan the probe scans the material surface in a flat plane over the material surface. In this scan the probe does not follow the object's surface contour. Hence, in this scan the air gap is non-uniform and varies greatly over the scan surface

- **No-tilt scan**

In the second type of scan, the no-tilt scan, the probe follows the surface, but is not always oriented perpendicular to the material surface. The probe lies parallel to the Z-axis of the fixed frame {F} at all times. Thus the surface at a given scan point (or specifically the tangent to the surface at a given scan point) could be at a relative angle other than 90 deg.

- **Full scan**

In this third type of scan, the probe follows the object surface with its orientation perpendicular to the object's surface through the scan, thus maintaining the probe perpendicular to the tangent to the surface at a given scan point.

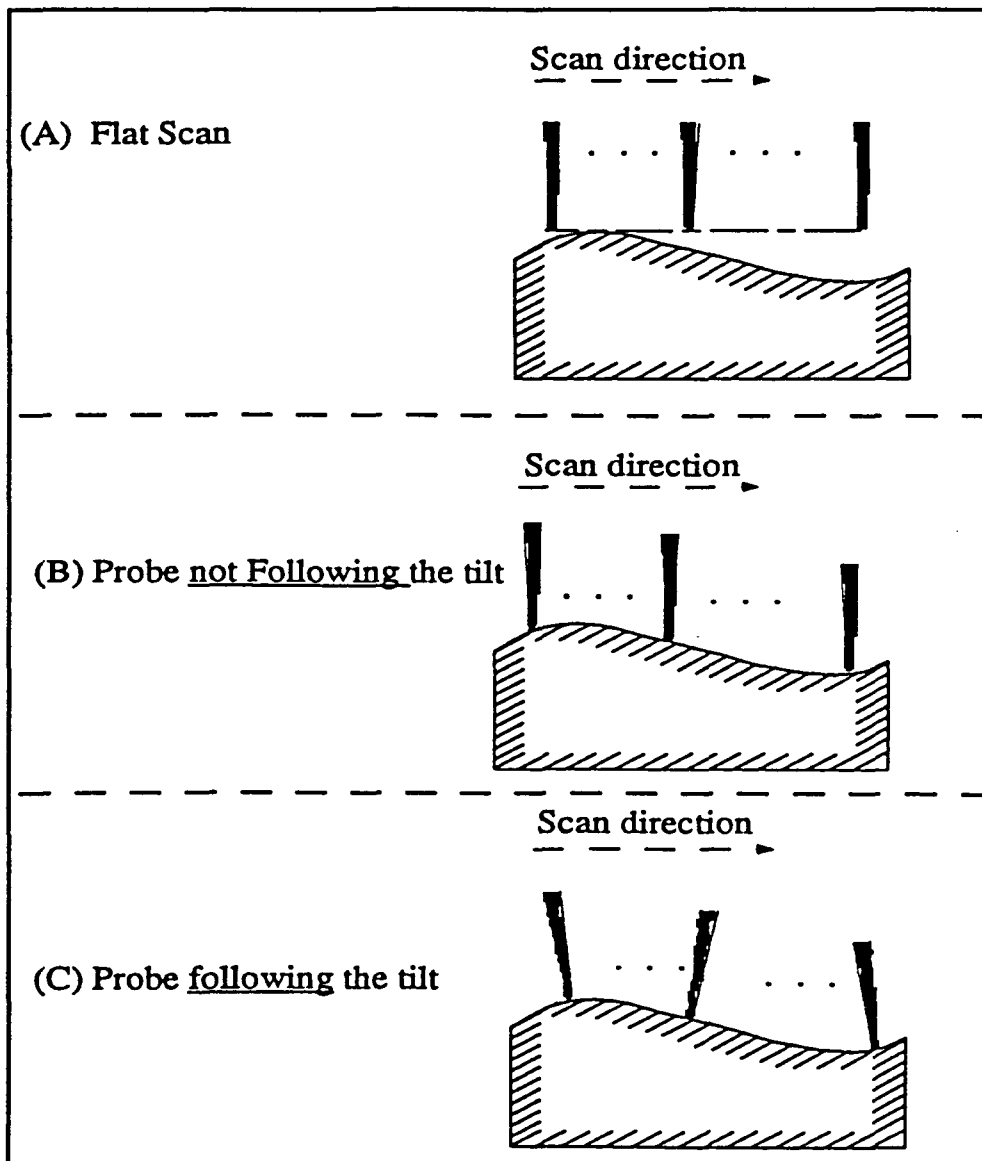


Fig. 6-3: The three different types of scans

6.2 Scan Results And Evaluation

This section describes the scans conducted on the two test pieces and the data obtained from these scans.

The data plots for block-1 are shown in Fig. 6-4, Fig. 6-6 and Fig. 6-6. The figures provide three dimensional view of the impedance data as it varies over the surface of the object. The first two figures show the impedance plot for “flat” and “no-tilt scans” respectively (for scan types, see 6.1.2). As is seen from the data plots the background data surface in these two plots is not flat; the background signal presence is very clear in Fig. 6-4 where the lift-off variation is very drastic, as the probe scans the surface in a flat plane only. In the case of Fig. 6-5, the probe attempts to follow the surface, but does not orient itself perpendicular to the surface at the scan point. In both cases, there exists a relative non-perpendicular orientation between the probe and the sample surface at the scan points (as the probe is not constrained to be perpendicular to the scan point).

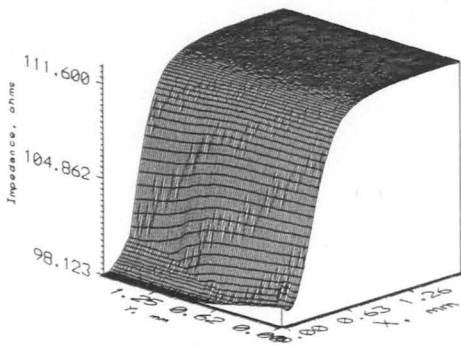


Fig. 6-4: Block-1. no-tilt scan - real part

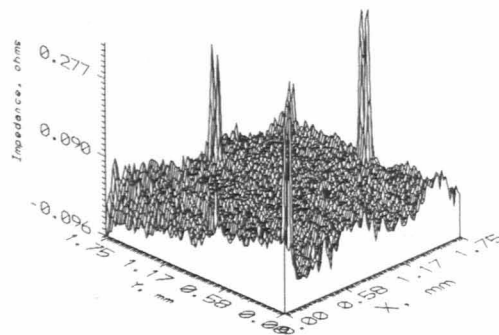


Fig. 6-5: Block-1. Not-tilt - Imag. part

In the above scans only the 40mil. wide notches are detectable. In the no-tilt scan the 40mil EDM notches were easily seen (after noise and background subtraction), while hardly any flaw signal is seen in the case of the flat scan. Now, Fig. 6-6 shows the impedance plot for block-1 with the probe perpendicular to the object surface. To orient the probe perpendicular to the curvature, the post-processor program calculates the probe and object translation and rotation angles such that the probe is always perpendicular to the material surface at all the scan points. The object is also rotated where probe rotation alone does not result in the probe achieving a perpendicular orientation. As is seen, the data from the scan reveals two sets of EDM notches (40mil. and 20 mil wide EDM notches) much more clearly than the previous data (Fig. 6-4 and Fig. 6-5).

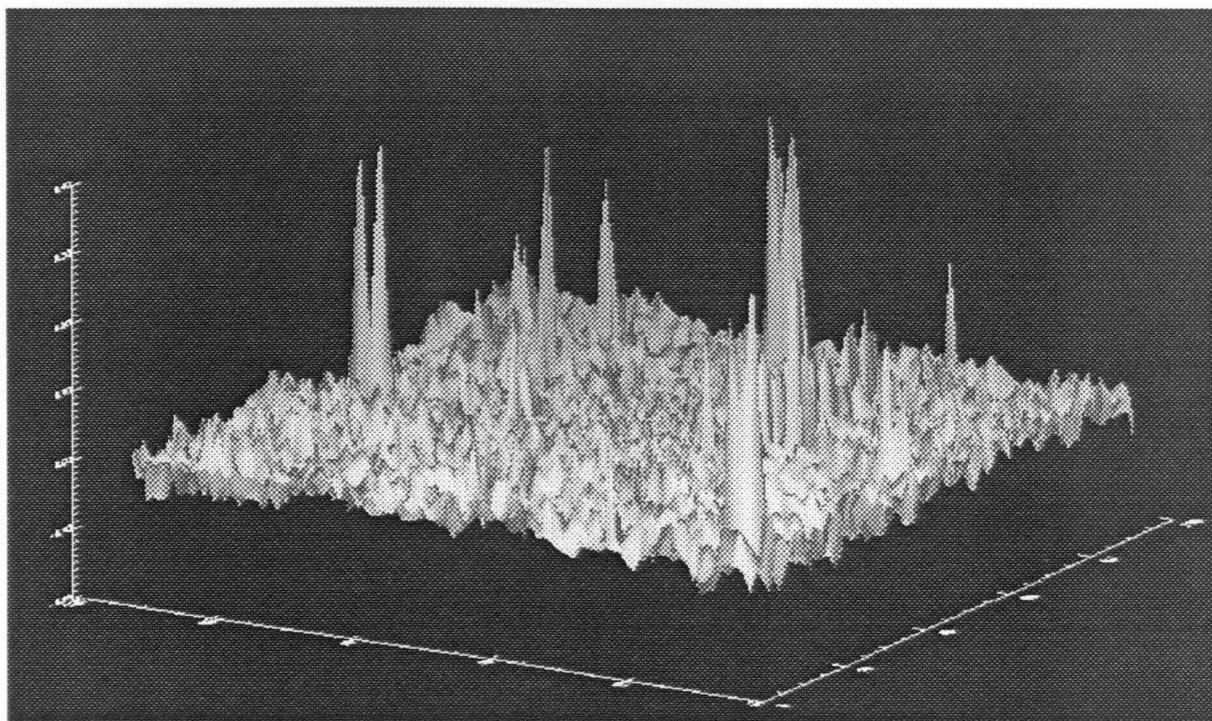


Fig. 6-6: Block-1 - complete scan

The next three plots pertain to the flat, no-tilt and full scan for block-2. Comparing the three plots clearly demonstrates the effect of probe tilt. In this case too the background data hides the flaw data effectively in the case of the first two types of scan. The relative probe-sample non-perpendicularity is seen as a non-planar background in Fig. 6-7 and Fig. 6-8. In Fig. 6-9, however, the probe is maintained at a perpendicular orientation to the object surface at all times and as expected, the background is a flat plane. In this case the signals from the notches are clearly visible, with even the smallest set of EDM notches being seen (10mil).

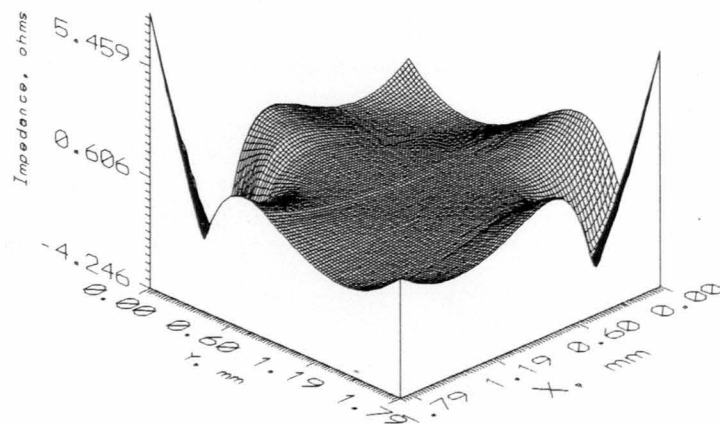


Fig. 6-7: Block-2 - Flat scan

It is interesting to note the effect of the background on the data collected. The variation in the background is much more pronounced when the probe scans the surface in a flat plane. Here (Fig. 6-7), the air gap varies widely over the entire scan surface, resulting in a very low probability of detecting the presence of a flaw (simulated here, by the EDM notches). In Fig. 6-8, the lift-off variation is limited by conducting the no-tilt scan.

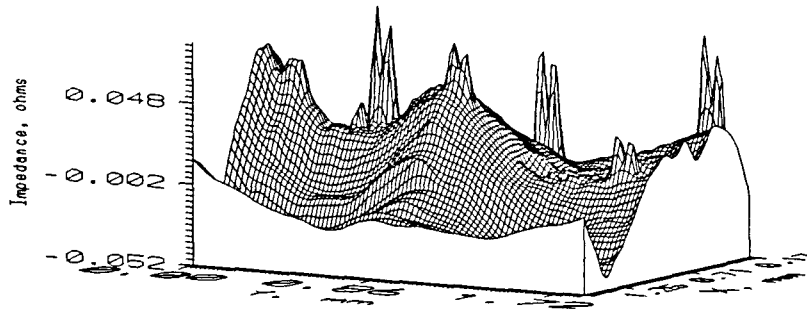


Fig. 6-8: Block 2 - no-tilt scan

In Fig. 6-8, the probe in scanning the surface attempts to follow the variation in the Z axis (of frame {F}), but always maintains a perpendicular orientation with respect to {F}. Thus the effect of the background is not as pronounced here as in case of the flat scan over block-2. Thus here, the bigger EDM notches could be detected by the probe clearly, but the smallest set of EDM notches still remain undetected as they are hidden by the non-planar background.

In Fig. 6-9, the probe follows the surface while maintaining its perpendicularity to the surface at all times. As expected and as seen in Fig. 6-9, the background is mostly planar. This is because the probe at all points essentially “sees” only a flat surface as it is positioned perpendicular to the surface. All the EDM notch signals stand out in this scan, with even the smallest notch being seen. In the case of Block-2, ensuring that the probe remain perpendicular to the surface requires the object to rotate too. Thus, scanning this block in particular, helps us in verifying the theory that the object rotation can indeed compensate for the lack of rotation of the probe.

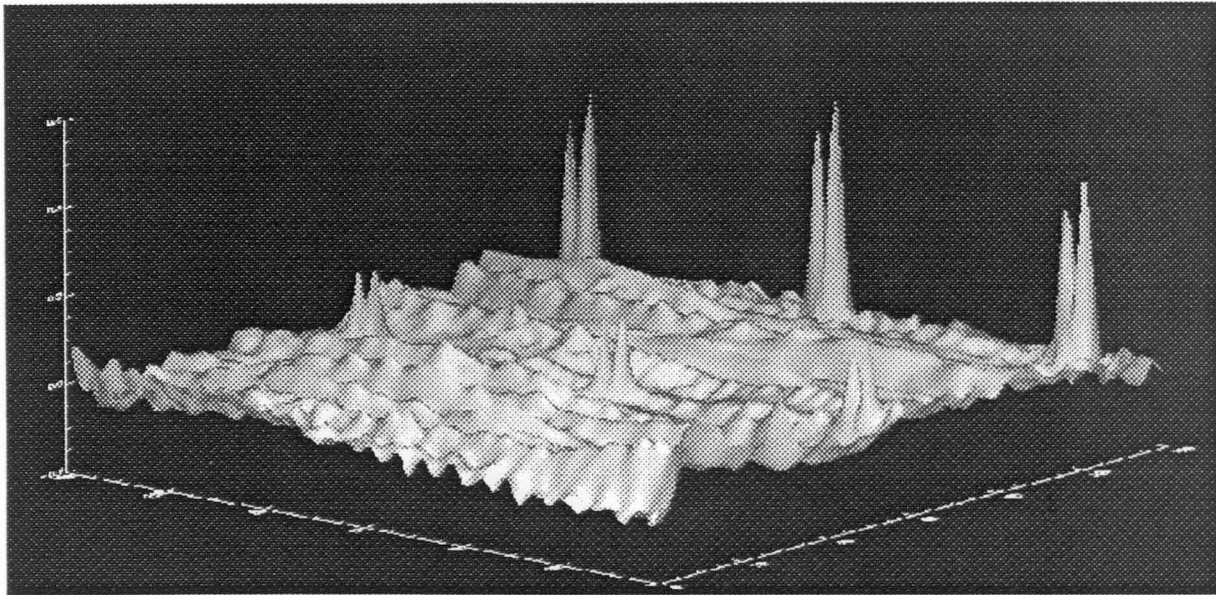


Fig. 6-9: block-2 - Complete scan with probe following curvature.

In summary the testing proceeded from the relatively simple uni-curvature of block-1 to the more complex double curvature of block-2. The single curvature scan required hardly any object rotation as the probe could rotate in one plane and this is sufficient to handle such scans. In the case of the double curvature scan the object had to be rotated too as the nature of the surface otherwise required that the probe be able to rotate in at least two planes. Tests were conducted on these objects and data sets from the scans on the objects showed the very high sensitivity of the probe to relative surface orientation. It was seen that a perpendicular orientation produced a mostly planar surface over which the flaw signals clearly stood out, thus increasing the probability of detection.

7. SUMMARY AND CONCLUSIONS

Eddy current inspection is very sensitive to changes in lift-off of the probe from the sample and to the orientation of the probe with respect to the sample. Positioning the probe perpendicular to the sample is a task that is a function of object geometry. This work concentrated on the development of a motion algorithm to automate the probe positioning process, so that given any object it is possible to maintain probe perpendicularity and constant lift-off over all the scan points.

Developing motion control software with object geometry features embedded in it limited the scope of applications and reusability of that software. Further, developing object specific custom software to control the scans resulted in unnecessary time spent in code duplication as many abstract features were reimplemented. Also, developing such code was a programmer subjective process and more open to the possibility of errors each time a scanning software was developed. All the above factors were addressed by the development of a postprocessor algorithm that takes in the scan parameters generated by a CAM software and determines the exact motions needed by the probe and object.

By developing an algorithm to determine the component motions of the scan, the scanning software was partitioned from the particulars of the motions for a scan (which are dependent on the geometry of the object being scanned). Object geometry information which was embedded earlier in the motion control software is now input to the algorithm at runtime. This development has resulted in cutting down the scan development time while not sacrificing the accuracy of measurements. With the development of the algorithm

(implemented as a postprocessor) the scanning process from the scan visualization to the scan realization has been integrated. It is now possible to realize a (software) visualized scan by manipulating the hardware, without having to develop any object specific scanning programs. The use of CAD/CAM tool path generation provides the scan visualization features, that allow easy and user-friendly modifications to scan paths, providing more flexibility in the scan conception stage. Thus in summary, when a given object needs to be scanned, a software scan plan using visualization aids is first developed. The scan plan is then used by a postprocessor that generates hardware specific probe and object rotations so that these (hardware) motions result in the probe being positioned perpendicular to the object at each of the scan points.

This work was organized in the following manner. Chapter 2 provided a brief introduction to eddy current theory. Chapter 3 described the three main hardware components, namely the positioning hardware, the measuring unit and the control unit. The latter three components formed the eddy current testbed site that executes the actual scan. Chapter 4 described the eddy current inspection process and described the experimental module of this inspection process. The automation of this experimental module formed the main focus of this work.

Chapters 5 described in detail the design of the post-processor algorithm (that automates the experimental module) and its characteristics. Chapter 6 discussed the types of scans performed, to test the utility of the algorithm and highlighted the need for maintaining probe perpendicularity and constant lift-off through the course of a scan. Results from experiments on two test blocks with embedded flaws were presented.

7.1 Suggestions for Future Work

The solutions derived for the rotation of the probe and the object (Chapter 5) are not order dependent. This feature could be exploited to parallelize the individual motions, reducing the time taken reach the “target position”. This would however, require care to ensure that there is no probe and object interference during the course of the motion. Also, if the current “stop” and “go” method of data acquisition is replaced with an “on the fly” method, it would reduce the total scan time. Another improvement that would be clearly helpful, is the development of a method to uniquely map the probe position of on the software to the physical point on the object. Currently, this mapping is done using a trial and error process and is susceptible to human errors. The current implementation of the data acquisition system is a sequential process running under a single tasking operating system.

The power of automated scanning can be further enhanced, by porting the software to run under a multi-tasking operating systems. This feature will free the computer from being tied up in scan control and allow for more efficient use of existing computing resources. Integration of the computer to a network of work stations will further improve scan efficiency by allowing concurrent data visualization, scan control (start, abort etc.) or scan status monitoring from other remote sites via the internet.

BIBLIOGRAPHY

- [1] Fu K.S., Gonzalez R.C, Lee C.S.G., "Robotics: Control, Sensing Vision and Intelligence", McGraw-Hill Book Company, Singapore, 1988.
- [2] Craig, J J., "Introduction to robotics", Addison-Wesley Inc., Reading, Mass., 1989.
- [3] Hagemaiier, D.J., "Fundamentals of Eddy Current Testing", The American Society of Nondestructive testing, Inc., Columbus, Ohio, 1990.
- [4] Blitz J., "Electrical and Magnetic methods of Nondestructive Testing", Adam Hilger, Bristol, N.Y, 1991.
- [5] Victor C., "An Introduction to Laboratory Automation", Wiley, New York, N.Y, 1990.
- [6] Bugar A.I., "Software Design and Implementation of a Contactless Surface Sensing NDE Scanning System", M.S. Thesis, Iowa State University, Ames, 1993.
- [7] Auld B.A., Jefferies SR., and Moulder J.C., "Eddy-Current Signal Analysis and Inversion for Semielliptical Surface Cracks", J. of Nondestr. Eval., Vol. 7, 1988, p 79.
- [8] Auld B. A, Muennemann F.G., Riazat M., "Quantitative Modeling of Flaw Response in Eddy Current Testing", Vol. VII, Research Techniques in Nondestructive testing, Academic Press, London, 1984.
- [9] Bugar A.I. and J.C. Moulder, "Use of Eddy current sensors for controlling lift-off actively during scans", Review of progress in Quantitative Nondestructive Evaluation Vol. 13, 1994, p 1103.
- [10] Kernighan B.W., Ritchie D. M, "The C Programming Language", Prentice Hall of India Pvt. Ltd., New Delhi, 1988.

- [11] "Operation Manual for the Model 4194A Impedance Gain-Phase Analyzer", Yokogawa-Hewlett Packard, Ltd., Tokyo, Japan, 1986.
- [12] "Compumotor, Model 4000 Indexer user Guide", Parker Hannifin Corporation, Rohnert Park, California, 1993.
- [13] "NI-488.2, Software Reference Manual for MS-DOS/MS-WIN", National Instruments Corporation", Austin, Texas, 1992.
- [14] "Mastercam 386 mill reference manual, ver. 4.00", CNC Software, Inc., Tolland, Connecticut, 1992.